UNIVERZITA KARLOVA V PRAZE
Přírodovědecká fakulta

Studijní program: Biologie
Studijní obor: Buněčná a vývojová biologie

Bc. Daniela Glatzová

Lokalizace koreceptoru CD4 a jeho variant v lidských T buňkách
Localization of CD4 coreceptor and its variants in human T cells

Diplomová práce

Školitel: Mgr. Marek Cebecauer Ph.D.

Praha, 2013

Prohlášení

Prohlašuji, že jsem závěrečnou práci zpracovala samostatně a že jsem uvedla všechny použité informační zdroje a literaturu. Tato práce ani její podstatná část nebyla předložena k získání jiného nebo stejného akademického titulu.

V Praze, 06. 05. 2013

Daniela Glatzová

First of all I would like to thank to my supervisor Mgr. Marek Cebecauer, Ph.D. for his valuable advice and suggestions and also for his excellent and patient leadership. I would like to thank also to Mgr. Tomáš Brdička, Ph.D. (laboratory of Leukocyte Signaling, IMG AS CR) for all his help and helpful advice and for a chance to work in his lab. Last but not least, I would like to thank to my parents for their love and support during my studies.

Abstract

CD4 co-receptor of main T cell receptor (TCR) is essential for proper development of T lymphocytes and their function in adaptive immune responses. It is believed that CD4 stabilizes the interaction of TCR with antigenic ligand, peptide-MHC, and thereby improves T cell-dependent responses during immune reaction. CD4 is transmembrane glycoprotein with a number of structural motifs in its intracellular domain which do not dramatically affect its sorting to the plasma membrane but can influence its local organization at nanoscale. CD4 was shown to transiently accumulate in the immunological synapse formed between T cell and antigen-presenting cell. Such accumulation is rapidly followed by its internalization and/or delocalization outside the synapse. This is in contrast with TCR which accumulates strongly in the immunological synapse and is later found enriched in the central area of this structure. It is therefore unclear how TCR and its CD4 co-receptor function together when binding to their common ligand during the initiation of signaling in T cells.

We aim to study localization of CD4 at nanoscale using advanced fluorescence microscopy techniques achieving significant improvements in resolution. In this work, CD4 and its mutant variants, potentially causing its different localization at the membrane, were fused with fluorescent proteins and characterized. All constructs were confirmed to yield in expression of expected recombinant proteins which were localized to the plasma membrane and intracellular vesicles in human T cells. The constructs with photoconvertible fluorescent protein were further tested in localization microscopy.

This work succeeded in generation and thorough characterization of plasmids encoding CD4 and its mutants required for further work focused on precise localization of these molecules at the surface of activated T cells. Such knowledge can help to understand relation between TCR and CD4 during the early phase of T cell activation, yet further investigation will be required to clarify dynamics of immune synapse formation, and thereby the T cell activation.

Key words: T cell, T cell receptor, CD4 co-receptor, immune synapse, superresolution microscopy

Abstrakt

CD4 je koreceptorem T receptoru nacházejícího se na povrchu T lymfocytů. Jedná se o glykoprotein z rodiny transmembránových proteinů. Jeho přítomnost je nezbytná jak pro vývoj T lymfocytů, tak i pro jejich správnou funkci. Předpokládá se, že CD4 stabilizuje interakci T receptoru s jeho ligandem, MHC-peptidovým komplexem, a tím přispívá k imunitní odpovědi založené na T buňkách. Vnitrobuněčná část CD4 obsahuje řadu strukturních motivů, které většinou neovlivňují umístění proteinu v plasmatické membráně, ale mohou významně ovlivnit jeho umístění v rámci domén, které se v plazmatické membráně T lymfocytů tvoří. Ukázalo se, že se CD4 přechodně hromadí v místech interakce T buňky a antigen-prezentující buňky, nazvaných imunologická synapse. Krátce po nahromadění CD4 koreceptoru v imunologické synapsi je buď vyloučen z místa, kde se imunologická synapse vytvořila, nebo úplně odstraněn z plasmatické membrány. Tento jev je v nesouladu s chováním T receptoru, který se po vzniku imunologické synapse hromadí v její centrální části. Z tohoto důvodu zůstává nejasné, jakým způsobem CD4 koreceptor a T receptor spolupracují při vazbě MHC-peptidového komplexu během zahájení T buněčné signalizace.

Naším cílem je studium umístění CD4 koreceptoru na plasmatické membráně s použitím pokročilých mikroskopických metod, které zajišťují podstatné zlepšení rozlišení obrazu v nanometrovém měřítku. V této práci byly kromě lidského CD4 použity i jeho mutantní formy, které by mohly jeho umístění v rámci plazmatické membrány ovlivňovat. Všechny CD4 varianty byly úspěšně spojeny s fluorescenčními proteiny a ocharakterizovány. Exprimované proteiny se nacházely především v plazmatické membráně a částečně i v membránách cytozolických váčků. Ty konstrukty, které byly vytvořené spojením s fotokonvertovatelným fluorescenčním proteinem, byly navíc ocharakterizované pomocí lokalizační mikroskopie s vysokým rozlišením.

Znalosti, získané z lokalizační studie CD4 nám pomohou lépe pochopit vztah mezi koreceptorem a T buněčným receptorem během aktivace T buněk. K objasnění dynamiky vytváření imunologické synapse a tím i pochopení T buněčné odpovědi bude však zapotřebí dalšího výzkumu.

Klíčová slova: T buňka, T buněčný receptor, CD4 koreceptor, imunologická synapse, mikroskopie s vysokým rozlišením

Content

1 Introduction

The major function of immune system is to protect the organism from environmental agents such as microbes and viruses, to detect and eliminate damaged and tumor cells and distinguish those from healthy cells and tissues to preserve the integrity of the body. Numerous biological structures and processes form this highly complex system.

Human immune system consists of two major types of immunological responses, the innate immunity also known as non-specific response and adaptive immunity also known as specific response.

Innate immune system is evolutionary older defense strategy found in many organisms. It is the first immune response activated immediately after pathogen recognition. The innate immune system is composed of cells and mechanisms recognizing simple molecules and regular patterns of molecular structures such as mannose-rich oligosaccharides, peptidoglycans and lipopolysaccharides from the bacterial cell wall. Innate immunity is non-specific and does not lead to a long-term immunity or immunological memory. Human innate immune system functions also in recruiting immune cells such as natural killer cells, mast cells, macrophages and other leukocytes to the site of infection, activation of complement system and subsequent activation and regulation of the adaptive immune responses (Hořejší and Bartůňková, 2005).

Adaptive immune system provides organisms with the capacity to distinguish and remember specific pathogens throughout the life. It is the second line of defense stimulated by innate immune system and, therefore, such response to pathogenic infection may take several days. The adaptive immune system is characterized by the production of antibodies (soluble proteins that bind foreign antigens; antigen is a substance that, when introduced into the body, is capable of stimulating an immune response, specifically activating lymphocytes) and cell-mediated responses in which specific cells recognize modified cells. Cells of the adaptive immune system are T and B lymphocytes (T and B cells). In contrast to innate immune cells, specific memory T and B cells can develop after encountering with the pathogen. T and B cells have different roles and types of antigen receptors (Hořejší and Bartůňková, 2005).

In B cells, an antigen binds to B cell receptor (BCR) on their surface, inducing lymphocyte proliferation and differentiation into plasma cells. Plasma cells are effector forms of B lymphocytes that produce antibodies which are a secreted form of the B-cell

receptor and have identical antigen specificity. Unlike B cells, T cells recognize antigens present on the surface of cells by MHC (major histocompatibility complex) molecules. Recognition and binding to the MHC-antigen complex is mediated by TCR (T cell receptor), transmembrane receptor on the surface of T cells. After activation, T cell proliferates and differentiates into one of several different functional types of effector memory T lymphocytes (Murphy et al., 2008). Since this work is focused on the organization of molecules at the surface of T cells in general, only two main subtypes, effector CD4+ and CD8+ T cells will be discussed in more detail in the following text.

1.1 T cells

T cells are white blood cells essential for the immune system function in vertebrates. T cells are generated from common lymphoid progenitor in bone marrow. They mature and develop in an organ called thymus. Matured T cells travel to secondary lymphoid tissues such as lymph nodes and lymphoid follicles. A smaller number circulates in the blood.

When entering thymus, lymphoid precursor cells express various TCR forms and CD4 or CD8 glycoprotein molecules on their surface required for their function. In thymus, T cell receptor precursor pre-TCR, TCR, as well as CD4 and CD8 molecules appear on their surface during specific phases of T cell maturation. Here, T cells come into contact with MHC class I and MHC class II molecules (major histocompatibility complex I and II), their natural ligands. MHC I and MHC II molecules are protein complexes specialized to carry self or foreign peptides and present those to the T cells. They are located at the surface of APCs (antigen presenting cells) such as dendritic cells, macrophages, and B cells. In thymus, immature T cells recognize and bind either MHC I or MHC II molecules to survive (positive selection). Remaining T cells unable to bind MHC molecules undergo programmed cell death called apoptosis. T cells binding MHC II develop into CD4+ T cells, those binding MHC I into CD8+ T cells. The last phase of maturation is elimination of T cells which bind to self-antigens too strongly and, therefore, are potentially autoreactive (negative selection). T cells binding peptide-MHC (p-MHC) complex too strongly in thymus undergo apoptosis. Surviving selected T cells travel out of the thymus

and form the available pool of naive T cells (Luckheeram et al., 2012; Laky and Fowlkes 2005).

By activation in the periphery, CD8+ T cells develop into cytotoxic T cells that kill cells infected with viruses or other intracellular pathogens and especially cancer cells. CD4+ T cells develop into several types of effector CD4+ T cells that provide essential additional signals activating or modulating antigen-stimulated B cells to differentiate and produce antibodies as well as enhance innate immunity response. These two subtypes of T cells CD8+ and CD4+ tightly cooperate during immune response (Luckheeram et al., 2012).

1.1.1 Cytotoxic CD8+ T cells

Intracellular parasites like viruses but also some type of bacteria multiplies in the cytoplasm of cells. These pathogens are not accessible by antibodies and the only way to eliminate of such infection is controlled destruction of these cells. Virus-infected cells display fragments of viral proteins as p-MHC I complexes on their surface. Cytotoxic T cells bind to the p-MHC I complex and recognize this type of infection. Cytotoxic T cells are able to kill these targets by inducing their apoptosis (Waterhouse et al., 2004). Apoptosis is preferable cell death to necrosis. During apoptosis, a cell is degrading itself from inside. Nuclear membrane is dissolved, DNA is fragmented and cell is shrinking into membrane bound vesicles which are eliminated by macrophages. This type of cellular death causes degradation of viral particles and intracellular bacteria together with cell body. During necrosis intact pathogens can be released and infect healthy cells (Murphy et al., 2008).

Cytotoxic T cells can kill target cells employing two major pathways. First, they express the death-inducing molecule Fas ligand (FasL) on their cell surface and this molecule, upon interaction with its receptor Fas, activates a suicide pathway in the target cells (Brunner et al., 2003). Second is calcium-dependent release of specialized cytotoxic granules. Cytotoxic T cells have unique cytoplasmic granules containing effector molecules with cytolytic activity such as perforin, granzymes and granulysin. Once cytotoxic T cells have come into close contact with their target cells by forming the immunological synapse (see below), they exocytose their granular content. Perforin molecules integrate into target plasma membrane and form pores. Perforin pores open a port for the entry of granzymes and granulysin that are released from the granules and

subsequently induce apoptosis in the target cells. In this way, these two killer mechanisms achieve cell destruction in a most efficient way. Cytotoxic T cells kill infected targets with great precision with a minimum tissue damage (Griffiths, 1995).

1.1.2 CD4+ T cells

Naive CD4+ T cells can differentiate into number subsets of effector T cells with different immunological functions. The main CD4+ T cell effector subsets currently distinguished are T_H1, T_H2 and T_H17 (T helper cells), which activate their target cells, and the regulatory T cell subsets that have inhibitory activity limiting the activation of immune system (Luckheeram et al., 2012), These subsets, particularly T_H1, T_H2 and T_H17, are defined on the basis of different cytokines they secrete (cytokines are small soluble proteins secreted by a cell that can alter the behavior or properties of target cells or itself). Most cytokines produced by T cells are given the name interleukin IL followed by a number and can have multiple biological effects (Glimcher and Murphy, 2000).

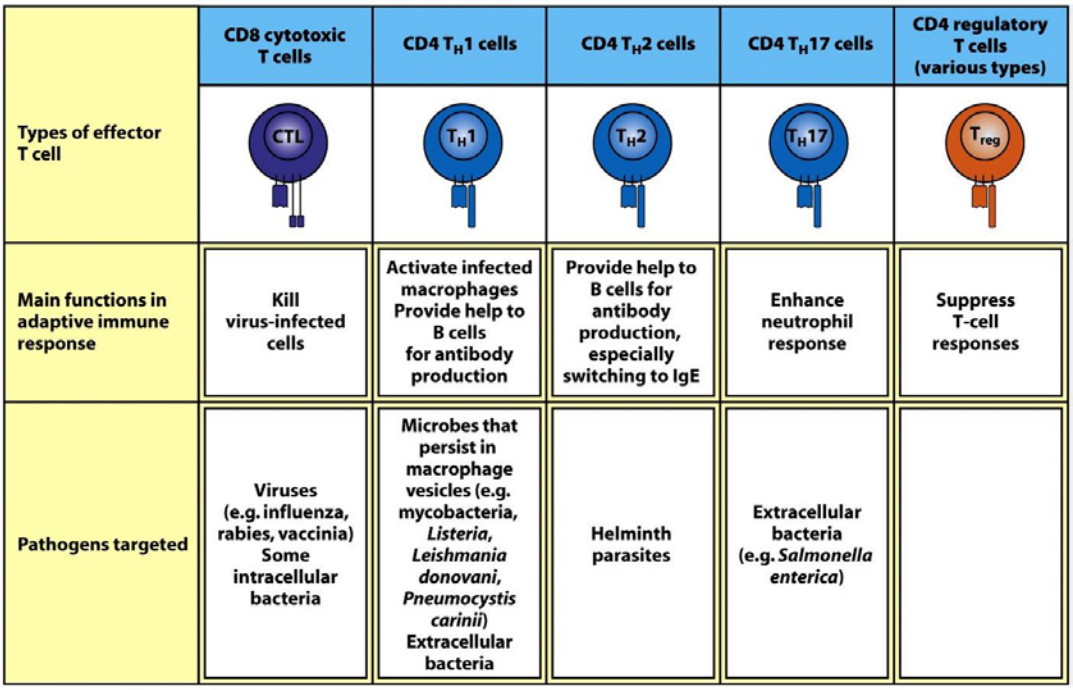

Fig. 1 Schematic representation of CD8+ and CD4+ T cell subsets. Derived from Murphy et al., 2008.

1.1.2.1 T_H1 CD4+ T cells

T_H1 cells have a dual function. One is to control bacteria that can set up intravesicular infections in macrophages, such as the mycobacterium causing tuberculosis and leprosy. These bacteria are taken up by macrophages in a usual way but can evade from the microbe-killing mechanisms of macrophages. If a T_H1 cell recognizes bacterial antigens displayed on the surface of an infected macrophage, T_H1 cells stimulate macrophages to increase the microbe-killing capacity of such cells. The other role of T_H1 cells is to stimulate the production of antibodies against extracellular pathogens by producing co-stimulatory signals for antigen-activated naive B lymphocytes. T_H1 cells also induce class switching of activated B cells to produce particular antibody isotypes. T_H1 cells mainly secrete IFNγ (Interferon γ) and TNFβ (tumor necrosis factor β, also known as lymphotoxin α). IFNγ is essential for the activation of macrophages thereby resulting in enhanced phagocytic activity (Luckheeram et al., 2012). TNFβ activates macrophages and is also involved in the formation of secondary lymphoid organs during development (Drutskaya et al., 2010).

1.1.2.2 T_H2 CD4+ T cells

T_H2 cells are similar to T_H1 cells in their capacity to induce immunoglobulin class switching of activated B cells to produce particular antibody isotypes. T_H2 cells are specific for the switch of B cells to produce IgE class of antibody important in parasite infection (for example helminthes). T_H2 cells play a major role in the induction and persistence of asthma, as well as other allergic diseases. The key effector-cytokines of T_H2 cells include IL4, IL5, IL9 and IL13 (Okoye and Wilson, 2011). IL4 has pleiotropic functions. It is a major cytokine involved in host protection from parasitic helminthes, promotes growth of activated human B cells and induces IgE/IgG class switching in B cells. IL4 is also involved in allergic inflammation (Koyanagi et al., 2010). IL-5 mobilizes recruits and matures eosinophils (Okoye and Wilson, 2011).

1.1.2.3 T_H17 CD4+ T cells

T_H17 cells are activated in the early phase of adaptive immune response. They are able to produce cytokines IL17 and IL6 which act in activating and recruiting neutrophils to the sites of infection to clear extracellular bacterial parasites. T_H17 cells are responsible to mount immune response against extracellular bacteria and fungi. They are also involved in the generation of autoimmune diseases (Luckheeram et al., 2012).

1.1.2.4 Treg CD4+ T cells

The main function of Treg cells is to suppress T-cell responses. After clearance of pathogens, they negatively regulate the immune response, thereby protecting against immunopathology and maintaining tolerance. They produce inhibitory cytokines such as IL10 and TGFβ (Fehérvari and Sakaguchi, 2004). IL10 suppresses T cell responses directly by reducing the production of IL2, TNFα and IL5 by T cells but not all effects of IL10 are immunosuppressive. TGFβ similarly blocks T cell cytokine production, cell division and killing ability (Roncarolo et al., 2001).

1.2 T cell receptor

1.2.1 T cell receptor structure

T cell receptor has capacity to recognize highly variable pool of antigens. On the other hand, individual T cells bear thousands of identical antigen receptors on its surface. There are several clones of T cells in the body expressing receptors with different specificity. Following text will describe only the most common αβ T cell receptor.

TCR consist of two different polypeptide chains termed T cell receptor α (TCRα) and T cell receptor β (TCRβ) linked by disulphide bond. T cell receptor has one antigen-binding site. The extracellular portion of both chains, α and β, consists of two domains: amino-terminal variable (V) region, forming antigen-recognizing site, constant (C) region and a short segment containing a cysteine residue form disulphide bond formation.

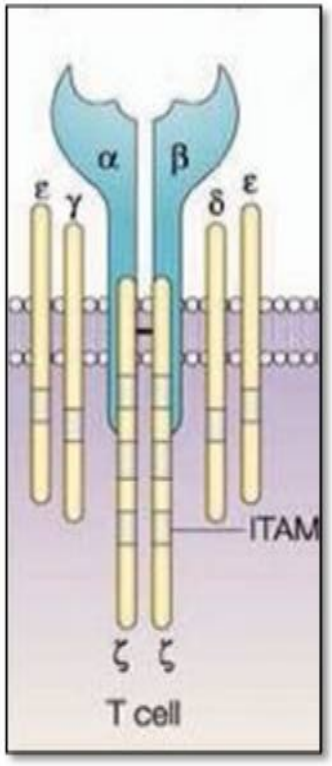

Fig. 2 Schematic representation of the T cell receptor complex, depicting subunits α, β, γ, δ, ε, $(\zeta)_2$. Derived from Manolios et al., 2010.

Each chain has transmembrane part and a short cytoplasmic domain. The transmembrane parts of both chains of T cell receptor contain positively charged (basic) residues within the hydrophobic segment (Weiss, 1990).

TCR binding p-MHC complex is unable to transmit signal itself. TCR forms multimeric receptor complex with four other signaling chain molecules of CD3 complex ε, δ, γ and ζ (Fig. 2). There are two ε, one δ and one γ chain called the CD3 complex. CD3 proteins have extracellular immunoglobulin-like domain (Ig-like), negatively charged transmembrane segment which associates with positive residues of αβTCR chains, and intracellular domain containing single ITAM (Immunoreceptor tyrosine-based activation motif) signaling motif. ζ chain forms covalently bound homodimer. It has a short extracellular part, intracellular domain containing three ITAM signaling motifs and a transmembrane domain with negatively charged residues associated with αβTCR (Call and Wucherpfennig, 2007). Formation of αβTCR-CD3 complex precedes sorting of TCR to the plasma membrane and its stabilization (Call et al., 2002). Signaling from the T cell receptor complex is due to the presence of ITAM motifs in CD3 ε, γ, β, δ molecules and ζ chains.

1.2.2 T cell antigen recognition

T cells detect the presence of pathogens on the surface of infected cells or APC in form of peptide fragments. These foreign peptides, together with self-peptides from endogenous proteins, are delivered to the cell surface by specialized protein molecules MHC I or II. MHC I and MHC II proteins are closely related but differ in subunit composition and type of binding partner molecules. Both helper and cytotoxic T cells use similar TCRs but typically respond to antigen associated with different types of MHC molecules.

1.2.2.1 MHC class I

MHC class I molecules are expressed at the surface of almost all nucleated cells in the body and present endogenous peptides to CD8+ T cells. The generally accepted model for MHC class I antigen processing is that peptides generated by proteolysis of cytosolic proteins, mainly by the proteasome, are translocated into the endoplasmic reticulum by the transporters associated with antigen processing (TAPs), where the peptides bind to newly assembled MHC class I (Cresswell and Howard, 1997).

MHC I is composed of two polypeptide chains, heterodimer of transmembrane bound α chain and microglobulin β_2 chain. α chain is composed of three domains α_1, α_2 and α3. α_1 and α_2 domains form peptide binding cleft where peptide is placed with both ends at either end of the cleft (Cresswell and Howard, 1997). Class I MHC molecules usually associate with peptides of 8-10 residues length in an extended conformation which enables direct interaction of peptide with TCR. Longer peptides are not absolutely excluded, they can bind either by extension of MHC I at the C-terminus or they can bulge out of the binding groove providing additional surface area for TCR recognition (Wilson and Fremont, 1993).

1.2.2.2 MHC class II

MHC class II molecules are expressed only at the surface of specialized APC and present antigenic peptides to CD4+ T cells. APCs include dendritic cells, macrophages and B lymphocytes. Peptides do not bind to class II in the endoplasmic reticulum of APC but instead are derived from proteins that have entered the cell via the endocytic way, following endocytosis at the cell surface. Thus the peptide repertoire of class II molecules

may include fragments derived from proteins of extracellular pathogens, such as bacteria (Weenink and Gautam, 1997).

MHC II protein is composed of two transmembrane glycoprotein chains, α and β. Each chain is composed of two domains: α1, α2 and β1, β2, respectively. Peptide binding cleft is formed by α1 and β1 domains. Class II MHC binding groove is open at either end so the length of peptides binding to MHC II is not constrained (Cresswell and Howard, 1997).

1.2.3 TCR activation

Several models for TCR mediated T cell activation have been proposed. One of those widely accepted in the past is monomer-co-receptor model first proposed by Janeway (1992). In monomer-co-receptor model, a single MHC II associates with a TCR and CD4 co-receptor. As the Lck kinase associates with the cytoplasmic tail of co-receptor molecules it can phosphorylates ITAM motifs of CD3 complex and ζ chains associated with TCR. This concept of T cell activation is abandoned due to the finding that initiation of signal transduction through TCR requires engagement of MHC-antigen complexes but no co-receptor (Boniface et al., 1998). Another T cell activating model called the pseudodimer model was proposed by Irvine and colleagues (2002). A single p-MHC complex could pair with TCR and cross link with CD4 co-receptor at the same time. This model suggests that the co-receptor CD4 can span an agonist-activated TCR to a neighboring (and very abundant) TCR that is engaged by a self-peptide–MHC complex and associated with active Lck. This would recruit the second TCR to the signaling complex and help the agonist-activated TCR to generate signals, thereby increasing sensitivity (Krogsgaard et al., 2005).

In case of CD8+ T cells restricted to class I MHCs, the role of endogenous ligand is not clear at this time. Earlier work suggested that endogenous pMHCs play no role in T cell activation (Spörri and Reis e Sousa, 2002). On the other hand, Cebecauer and colleagues (2005) observed similar stimulatory effect in CD8+ T cells.

1.3 TCR co-receptors

T cells make additional interactions with the MHC molecules that stabilize the interaction with TCR and are required for the T cell to respond effectively to antigen. These interactions are made through CD4 and CD8 transmembrane glycoproteins participating in T cell activation. During antigen recognition, CD4 or CD8 molecule associate with the TCR on the T cell surface and bind to invariant sites of the p-MHC complex (Zamoyska, 1998).

1.3.1 CD8 co-receptor

The CD8 molecule is a 34kDa surface glycoprotein expressed on CD8+ T cells. It participates in T cell development and activation. CD8 is a heterodimer consisting of α and β Ig-like chains covalently linked by a disulphide bond. The extracellular regions of the α and β chains of CD8 are similar to one another and consist of a single N-terminal Ig-like domain and a 50- (α) or 30- (β) amino acids long stalk region which links Ig domains to the plasma membrane. This extended polypeptide is highly glycosylated which protects it from cleavage by proteases. CD8 molecule contains short intracellular part through which it can associate with Lck (lymphocyte-specific protein tyrosine kinase; Src family kinase), kinase involved in TCR triggering. Unlike CD8β, CD8α chains can form homodimers (Leahy, 1995).

The CD8 binding site identified on MHC I molecule is located in a membrane proximal domain α3 of MHC I and contains several highly conserved negatively charged amino acid residues. Top face of the CD8 dimer contains several positively charged residues which interact with negatively charged residues within α3 domain of MHC I. Side face of CD8 dimer interacts with α2 domain of MHC I molecule (Giblin et al., 1994).

1.3.2 CD4 co-receptor

1.3.2.1 CD4 co-receptor structure

CD4 is a 55kDa cell surface glycoprotein expressed on CD4+ T cells participating in both, T cell development and antigen recognition by T cells. In addition, CD4 was demonstrated to function as a receptor for HIV (human immunodeficiency virus; Sattentau and Moore, 1993). CD4 is a single chain molecule passing once through plasma membrane (i.e. type I transmembrane glycoprotein). It was proposed that CD4 can form homodimers on the surface of T cells but the formal proof is still missing. It contains C-terminus in the cytoplasm and N-terminus extracellularly. Each CD4 co-receptor molecule contains four Ig-like extracellular domains, a transmembrane segment and a short cytoplasmic tail. First two Ig-like domains D1 and D2 are located at the distal N-terminus end of the CD4 molecule. They are packed together forming relatively rigid structure. CD1 and CD2 are connected with the two remaining Ig-like domains D3 and D4 with a short flexible hinge. D3 and D4 are packed together to form rigid structure similarly to D1 D2 (Leahy, 1995). The cytoplasmic tail of CD4 co-receptor contains several interacting structures (Fig. 3A). CD4 interacts with Lck via cysteines C445 and C447 and brings Lck molecule to the places where it can phosphorylate its targets such as ITAM motifs of CD3 complex and ζ chains. Therefore, it engages T cell signaling. CD4 molecule also contains basic rich motif with four arginine residues which gives the membrane proximal part of CD4 a positive charge. In the submembrane part of cytoplasmic tail, there are another two cysteines, C419 and C422, which are palmitoylated (Fragoso et al., 2003).

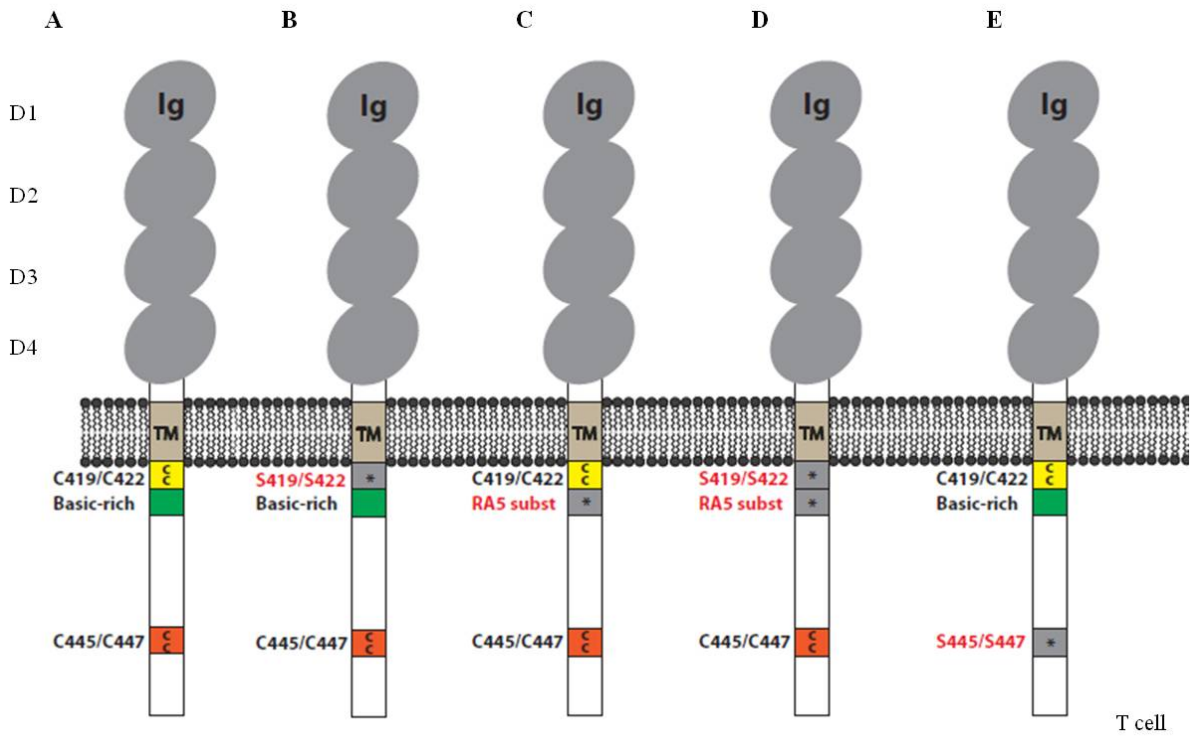

Fig. 3. Schematic picture of CD4 glycoprotein and its mutant variants used in this study.
D1-D4 - extracellular domains; TM – transmembrane domain; C419/C422 – palmitoylation site; basic-rich – RHRRR motif; C455/C447 – Lck binding site
A. CD4wt; **B.** C419/C422 mutated to serines S419/S422; **C.** RHRRR mutated to alanines AAAAA; **D.** combination mutant (B. and C.); **E.** C445/C447 mutated to serines S445/S447

1.3.2.2 CD4 interaction with MHC class II and TCR

The interaction between MHC II and CD4 is relatively weak. The primary CD4-binding site identified on MHC II molecules is in an exposed loop in a membrane proximal domain β2 of MHC II and contains several highly conserved negatively charged amino acids. CD4 is capable to bridge the length of a TCR and a portion of an MHC molecule to bring CD4 N-terminal D1 domain in contact with the membrane proximal domain of MHC II on APC surface (Leahy, 1995).

The TCR–p-MHCII–CD4 complex form arched-shaped structure. TCR binding p-MHC II complex is rather inclined than straight in trimolecular structure. D1 domain of CD4 co-receptor associates with β_2 domain of p-MHC II (Fig. 4). There are no direct contacts between TCR and CD4 in the TCR–p-MHCII–CD4 complex. There is wide separation between the membrane-proximal TCR α/β molecule and CD4 D4 domain (Yin et al., 2012). It provides enough space for the placement of TCR-associated CD3 εγ, εδ,

and ζζ subunits or cross-binding between two TCR-p-MHC II complexes as suggested by Krogsgaard and colleagues (Krogsgaard et al., 2005).

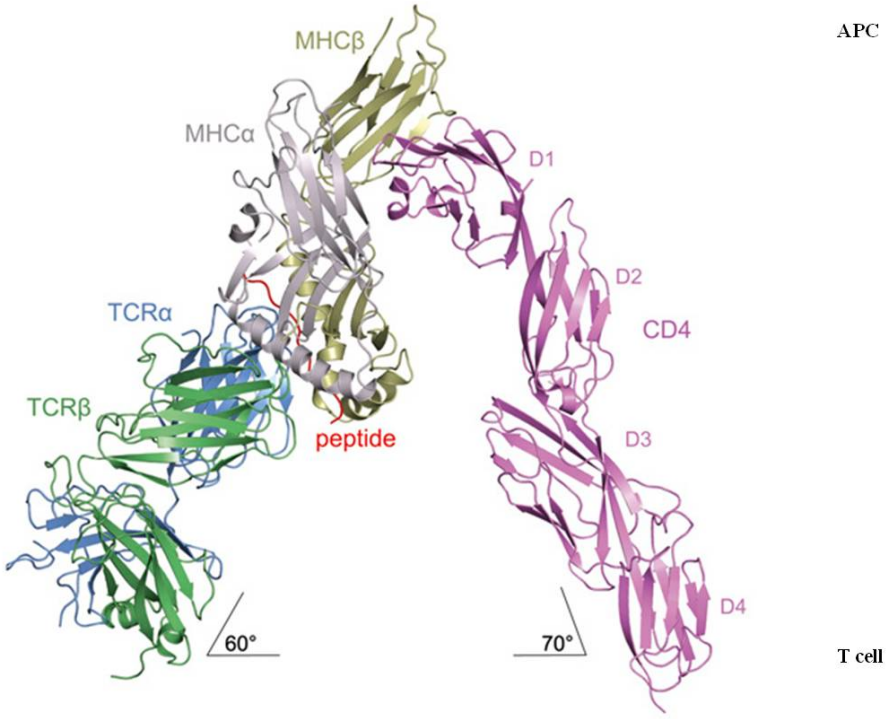

Fig. 4 Ribbon diagram representing TCR-p-MHCII-CD4 interactions. Adapted from Yin et al., 2012.

CD4 glycoprotein and its domains D1-D4 in violet; TCRα in blue; TCRβ in green; peptide bound by TCRαβ and MHCαβ in red; MHCα in grey; MHCβ in yellow.

1.3.2.3 CD4 mutant variants

Structure of CD4 co-receptor was intensively studied especially in 90s of 20th century due to its function as receptor for HIV. Mutational analysis of CD4 cytoplasmic tail ascertained several motifs. In my work, three of these motifs were examined. One of these motifs includes two C-terminal cysteines C445 and C447 essential for Lck binding. CD4 and Lck molecules associate due to cysteine coordination of Zn_2^+ ion (Veillette et al., 1988)[1]. Lck molecule is thought to stabilize CD4 co-receptor in plasma membrane. Laguette and colleagues tested this hypothesis introducing serine substitutions for C445

[1] It is important to note that numbering of CD4 amino acid residues used in my work could differ from those in cited articles. Numbering used in my work contains CD4 signal sequence of 25 residues according to protein database Uniprot (P01730; www.uniprot.org).

and C447 (C445, 447S mutant). Reduced amounts of C445, 447S mutant protein on T cell surface and increase internalization was observed (Laguette et al., 2009)[1]. Further revealed motif in the membrane proximal part of CD4 cytoplasmic tail was basic rich motif RHRRRR. When mutated to alanines (AAAAAA; RA5 mutant) CD4 changed localization to different membrane areas (soluble by Triton X-100; Popik and Alce, 2004). The main cause for the localization change could be the abolition of positive charge carried by arginine residues which interacted with polar heads of membrane lipids. Popik and Alce (2004) also studied palmitoylation mutation previously discovered by (Crise and Rose, 1992)[1]. There are two palmitoylated cysteines in the membrane proximal part of CD4 cytoplasmic domain, C419 and C422. It was supposed that acylation of specific amino acid residues could preferably recruit membrane proteins to specific domains. This assumption was supported by previous research (Melkonian et al., 1999)[1]. Unlike assumption, change of cysteines C419 and C422 to serines (C419, 422S mutant) did not affected CD4 localization in the detergent-resistant membranes. The purpose of CD4 palmitoylation remains unsolved.

1.4 The immunological synapse of T cells

The immunological synapse (IS) is the interface formed between an antigen-presenting cell or target cell and a lymphocyte such as T cell. Cytoskeletal changes are induced in T cells engaging antigen on the surface of APCs. Such cytoskeletal activity causes changes in T cell morphology and flattening of T cell on the surface of APC which occurs immediately after the initial recognition of antigen (Dustin, 2008). Simultaneously with the morphological changes, receptor-ligand complexes and signaling molecules involved in the adhesion and antigen recognition are organized into distinct domains or supramolecular activation clusters (SMACs; Grakoui et al., 1999).

The immunological synapse was initially defined as a stable cell-cell junction composed of three SMACs enriched in specific components. A central SMAC (cSMAC) containing kinases and clustered antigen receptors, a peripheral SMAC (pSMAC) abundant in β2 integrin adhesion molecule called LFA-1 (leukocyte function-associated molecule-1), and a distal SMAC (dSMAC) distinguished by the presence of tyrosine phosphatases (Fig.

5). However, recent studies suggest that formation of the IS is a highly active and dynamic process (Dustin, 2008).

In the IS, LFA-1 and talin are initially localized in contact area together with TCR segregated into small domains. After some time, in the order of a minute, this organization inverts so that TCR clusters to the cSMAC and LFA-1 and talin in the pSMAC (Grakoui et al., 1999). Distal SMAC (dSMAC) is an outer periphery ring of membrane enriched in CD45 (Freiberg et al., 2002).

The development of the IS includes cellular scanning, contact acquisition and adhesive arrest followed by early IS assembly and signaling, maturation and receptor segregation.

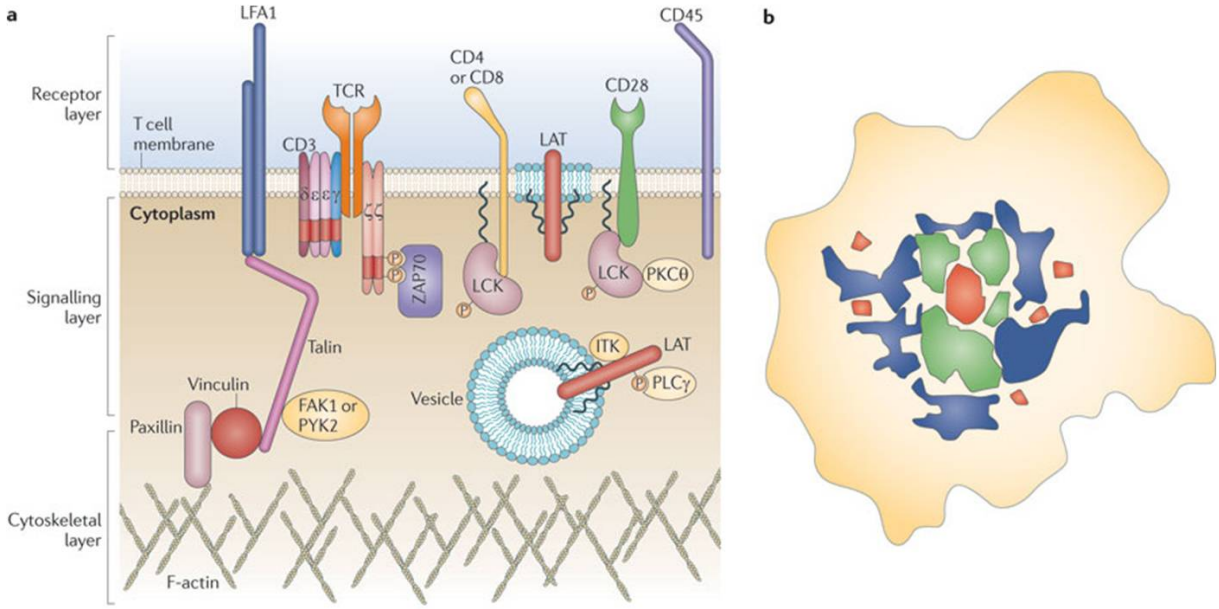

The process is finished by the TCR internalization and IS dissolution (Jacobelli et al., 2004).

Fig. 5 Schematic representation of T cell plasma membrane organization (a) and SMACs in the IS. Adapted from Dustin and Depoil, 2011.

a) Molecules involved in early TCR signaling.

b) The figure representing the arrangement of SMACs in the IS. cSMAC area rich in TCR is in red. Blue area represents LFA-1 rich pSMAC and intercalating green area of CD28 (provides co-stimulatory signals to TCR, it is involved in cytokine production (Nunès et al., 1996)).

1.4.1 Cellular scanning, contact acquisition and adhesive arrest

The first phase of the formation of the IS occurs when T cell moving over the surface of APC recognizes the antigen-MHCII complex. Antigen recognition by T cell results in a Ca_2^+ increase, which is sufficient and necessary to stop migrating T cell (Negulescu et al. 1996). Additional step contributing to the arrest of migrating T cell is the activation of LFA-1 molecule provided by TCR-MHCII-antigen recognition and subsequent binding of LFA-1 to its ligand ICAM1 (intracellular adhesion molecule 1) on APC (Dustin et al., 1997).

1.4.2 Immunological synapse assembly and signaling

In T cells, two protein tyrosine kinases of the Src family, Lck and Fyn, are thought to be responsible for the phosphorylation of ITAMs associated with TCR. Lck is mostly associated with the cytoplasmic domains of CD4 or CD8 co-receptors whereas Fyn associates weakly with the cytoplasmic domains of CD3 complex and ζ chains (Straus and Weis, 1992). The first step of TCR signaling is the activation of Src-family kinases. CD45 is a pivotal phosphatase in TCR signaling that has an essential role in priming of Lck for activation (Koretzky et al., 1990). Once phosphorylated by Lck (or Fyn), ITAM motifs form docking place for SH2 (Src Homology 2) domains of tyrosine kinase ZAP-70 (Zeta-chain-associated protein kinase 70) which activates and phosphorylates scaffold proteins LAT (linker of activated T cells) and SLP-76 (SH2 domain-containing leukocyte protein of 76kDa). These two adaptor proteins recruit PLC-γ (phospholipase C-γ) to the membrane. During several additional steps downstream signaling cascades are activated and calcium stores of the T cell are depleted (Schraven et al., 1999).

On the basis of early Ca_2^+ elevation, antigen receptors accumulate in the centre of the IS (cSMAC). The maintenance of the immunological synapse is important for continuous signaling and full activation (Grakoui et al. 1999). Application of new imaging techniques like TIRFM (total internal reflection fluorescence microscopy) to study the IS formed on functionalized supported planar bilayers revealed that signaling is maintained by the formation of TCR microclusters (MCs) that are continually formed at the periphery and transported to the cSMAC (Yokosuka et al. 2005). Both, the formation of the MCs and the transport of the MCs are actin dependent (Varma et al. 2006). These microclusters exclude

CD45. This exclusion zones may allow increased phosphorylation by tyrosine kinases in the cluster, including CD45 primed Lck that spread into the clusters from surrounding CD45-rich areas as recently demonstrated by Douglass and colleagues using single molecule imaging methods (Douglass and Vale, 2005).

1.4.3 The TCR internalization and IS resolution

In the last stage of T cell communication with APC, the TCR is internalized to the cytoplasmic vesicles in the cSMAC. The possible mechanism includes contact of CD45 phosphatase with TCR in cSMAC, therefore regression of signaling and accumulation of LBPA (Lysobisphosphatidic acid) in the cSMAC. The presence of LBPA in the cSMAC suggests that the cSMAC direct TCR into multivesicular bodies for degradation (Varma et al., 2003).

1.4.4 Role of CD4 in the IS formation

Optimal signaling through the T cell receptor complex occurs when it is associated with the co-receptor CD4. CD4 co-receptor is thought to stabilize the low affinity interaction between the T cell receptor and the MHC II antigen complex. Association of the TCR with co-receptor CD4 helps to stimulate signal transduction by bringing the Lck tyrosine kinase associated with CD4 to the proximity of ITAMs (Veillette et al., 1988; Rudd et al., 1989).

Despite numerous studies, the precise role of CD4 in the IS formation and function is not resolved. With CD4 capable to bind MHC class II molecules on the APC and bring Lck to the IS, initial models located CD4 co-receptor to the central region of T cell-APC contact (Kupfer et al., 1987). This view changed with live cell imaging of CD4 movement. Krummel and colleagues, using a T cell clone transduced with CD4-GFP (GFP-green fluorescent protein), found a transient accumulation of CD4 at the IS, where it accumulated at the c-SMAC for a couple of minutes, after which it moved to the periphery and further out of the synapse (Krummel et al., 2000). Lck was observed to move in a similar manner (Ehrlich et al., 2002). Thus, it is obvious that CD4 movement is a dynamic process at the IS, but how and why CD4 moves in and out of the IS is not known.

1.4.5 Superresolution microscopy

1.4.5.1 Superresolution techniques

One of major accomplishments in fluorescence microscopy was achieved when Abbe´s law (wavelength of light is a major limiting factor of image resolution) was circumvented by invention of nanoscopy visualization techniques. Unlike electron microscopy, nanoscopy can be used for living cells and therefore it's a method which can be widely used in imaging of dynamic structures and processes such as organization of molecules on plasma membrane. The main query of nanoscopy is to generate subdiffraction resolution images, which means improving spatial resolution by an order of magnitude or more over the diffraction limit (Huang et al., 2010).

There are a number of approaches in superresolution imaging techniques such as STED (stimulated emission depletion microscopy) method where non-linear physics is applied to improve resolution of imaging. STED is technique based on stimulated emission where deactivation (depletion) of fluorophores in doughnut shaped area using intense depletion laser light. The centre of this area is still emitting fluorescence due to excitation with lower intensity reading laser light. This circular area can be much smaller than the area excited using standard confocal setup (Hell and Wichman, 1994; Fig. 6).

Other superresolution techniques are STORM (stochastic optical reconstruction microscopy) and PALM (photoactivated localization microscopy), methods based on single molecule localization microscopy restricting a number of fluorophores emitting fluorescence simultaneously. The rest of fluorophores is kept in OFF state (dark). The distance between single fluorophores emitting in single frame has to be at least 5 times greater than the diffraction limit to distinguish individual molecules. This fluorophore switching enables software to determine the centre of each point with relatively good precision up to 10nm. High resolution image is generated from a large number of acquired frames (Fig. 6). The difference between STORM and PALM is that STORM technique uses small organic molecules fluorescence of which is controlled by different redox states (Rust et al., 2006). PALM technique employs proteins fused to photoactivatable or photoswitchable fluorescent proteins which do not emit fluorescence without activation or can emit at different wavelengths due to photoconversion, respectively. Emission in appropriate wavelength is achieved by activation/ photoconversion using low power UV

light to switch only limited number of fluorescent proteins at the same time (Betzig et al., 2006).

1.4.5.2 TIRF microscopy

TIRF microscopy is used to image fluorescent molecules and processes close to the optical glass. In TIRF microscopy, the laser beam illuminates the sample (e.g. cells on coverslip) under a high incident angle so that the beam is almost completely reflected from the glass /water interface. At so called critical angle (α) together with evanescent wave is generated which decreases exponentially with the depth of the sample. This evanescent wave excites only fluorophores near the glass/water interface (100-200 nm depth) which provides significant reduction of background noise fluorescence from the rest of the sample (Fig. 6A; Axelrod, 1981). This method is widely used simultaneously with PALM method imaging plasma membranes of cells.

1.4.5.3 Photoconvertible fluorescent proteins

PALM applied in this work uses unusual property of some fluorescent proteins, i.e. photoconversion. One of these proteins is mEOS2 (green to red photoconvertible protein EosFP). Common fluorescence proteins like GFP are emitting fluorescence constantly until they bleach. Photoconvertible proteins emit light at one wavelength (mEOS2 is green fluorescent protein) and while illuminated with UV light, they switch the fluorescence to emit at different (usually higher wavelength; mEOS2 switches to red). Similarly, PS-CFP2 (cyan-to-green photoswitchable fluorescent protein) emits very weakly in high UV spectrum but when photoconverted by low UV light it emits brightly in blue spectrum (similar to GFP). PS-CFP2 and mEOS2 emit at largely different wavelengths after photoconversion and therefore, can be used for two-color PALM in colocalization studies (McKinney et al., 2009; Chudakov et al., 2004).

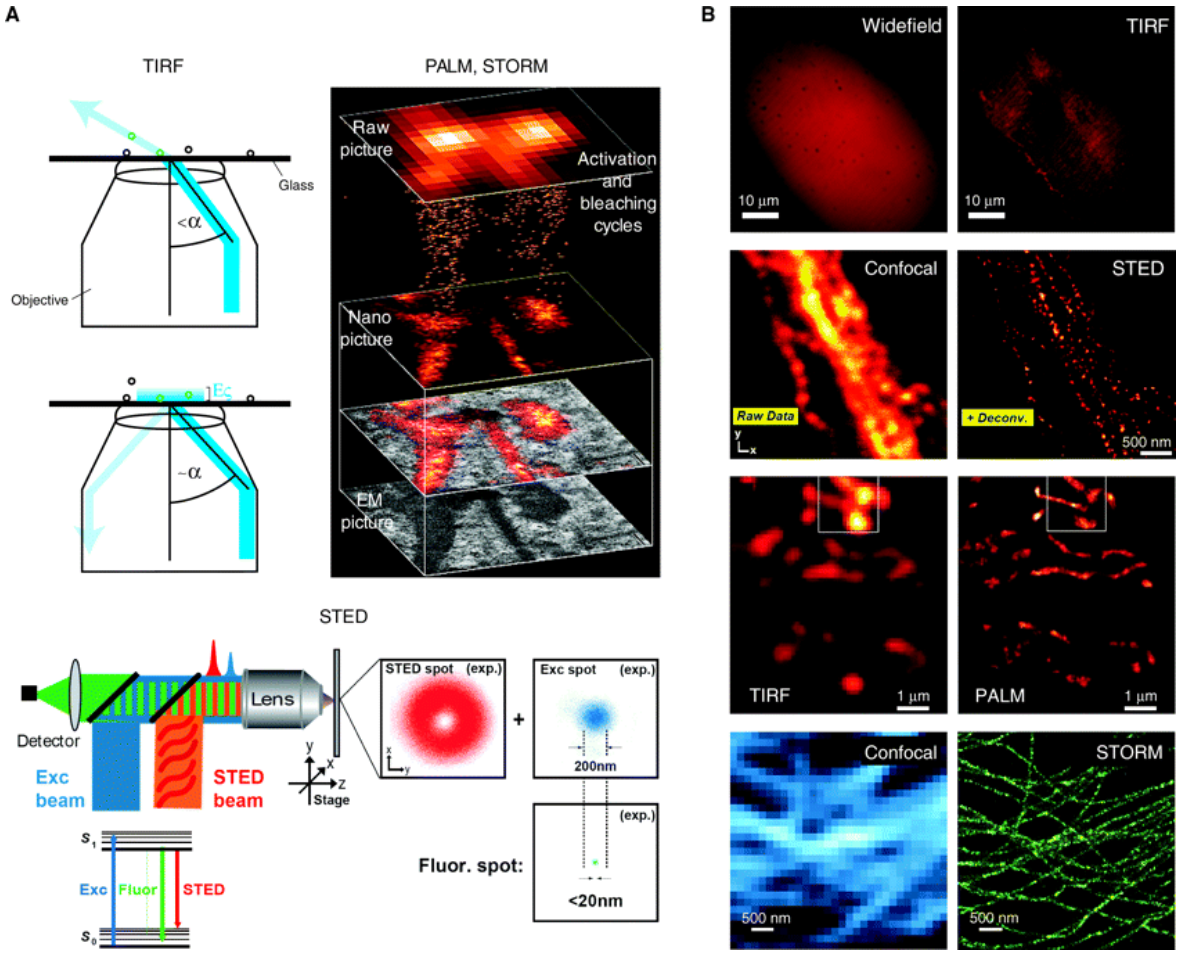

Fig. 6 Superresolution microscopy techniques. Adapted from Cebecauer et al., 2010.

A. On the left – Principle of TIRF microscopy.
   On the right – Scheme of PALM and STORM acquisition of high resolution images.
   At the bottom – Principle of STED technique.

B. Images acquired by conventional microscopy (confocal, widefield) compared to TIRFM, STED, PALM and STORM high resolution images.

1.4.5.4 Superresolution imaging of the IS

Immunological synapse is a very complex system consisting of many interacting proteins and is highly dynamic structure. Still it is not possible to observe dynamics of IS at nanoscale directly due to resolution restrictions of available microscopic techniques (Owen et al., 2010). PALM and STORM techniques with combination of TIRF microscopy offer increased resolution of studied protein interactions at the plasma membrane. Sherman and colleagues (2012) examined colocalization of LAT, TCRζ, ZAP-70 and some other molecules within the IS in both activated and resting T cells using two

color PALM. They observed both separated and mixed pools of LAT and TCRζ molecules at the plasma membrane in both activated and resting T cells which was in contrast to previous studies where LAT and TCRζ were observed in segregated domains before T cell activation and showing intermixed pattern after T cell activation (Lillemeier et al., 2010). Sherman and colleagues (2012) also identified microclusters with colocalization of LAT, ZAP-70 and TCRζ which they called "hot spots", i.e. places where ZAP-70 binding TCR complex phosphorylates LAT. They observed high dynamics of these microclusters within the IS. Equally interesting observation was made by colocalization of LAT, SLP-76 and polymerized actin. They also confirmed previous studies (Morley et al., 2006) about the importance of actin cytoskeleton in the IS dynamics and T cell function. In an article recently published Rossy and colleagues (2013) examined relation between conformational states of Lck and TCR signaling. They confirmed previously observed exclusion of CD45 phosphatase from microclusters containing phosphorylated TCR complex during TCR triggering (Douglas and Vale, 2005) and demonstrate that conformation of Lck forms clusters more frequently compared to the closed, inactive form. More studies are needed to uncover complexity of the IS at high detail and we intend to contribute to this aim.

2 Aims of the thesis

- Construction of EGFP/mEOS2 fusion variants of human CD4 protein
- Proper characterization of all generated constructs
- Validation of CD4 variants fused to mEOS2 photoconvertible protein for localization microscopy

3 Material and Methods

3.1 Material

3.1.1 Cells and bacterial strains

Cell lines:

- Jurkat E6.1 (derived from human T cell lymfoblastoma)
- HEK 293FT (derived from human epithelial kidney cells)

  - *cell line collection of Department of Leukocyte Signaling, IMG AS CR*

Bacterial strain:

- Escherichia coli – strain TOP10

  - *Invitrogen, Carlsbad, CA, USA*

3.1.2 Tissue culture media

- DMEM, RPMI 1640 and colorless RPMI 1640 media - supplied with 10% FBS (fetal bovine serum) with or without antibiotics (penicillin 100 U/ml, streptomycin 100 μg/ml, gentamicin 40 μg/ml), Opti-MEM media
  - *Invitrogen, Carlsbad, CA, USA*
- LB medium (without or with ampicillin or kanamycin 100 μg/l)
- LB agar (1.5 %) with ampicillin or kanamycin
  - *tissue culture media facility IMG AS CR, Prague, CR*
- FBS (fetal bovine serum)
  - *Gibco BRL, Paisley, UK*

3.1.3 Plasmids and primers

Plasmids:

- CD4wt1-EGFP/pEGFP-N1
- CD4CS1-EGFP/pEGFP-N1
- CD4RA5-EGFP/pEGFP-N1
- CD4CS1RA5-EGFP/pEGFP-N1
  - *kind gift of W. Popik (W.P., Meharry Medical College, Nashville, U.S.)*
- CD4wt2 /pCG
- CD4CS2 /pCG
  - *kind gift of S. Basmaciogullari (S.B., Institute Necker, Paris, France)*
- pmaxGFP
  - *Applied Biosystems, Foster City, CA, USA*
- pXJ41-LIME
  - *prepared by T. Brdička (Department of Leukocyte Signaling, IMG AS CR)*

PCR primers:

- designed in house and purchased from *Sigma-Aldrich*

	purpose	restriction site	Sequence 5´-3´
1	mEOS2 Fwd	BamHI	GAAGGATCCACCGGTCGCCACCATGAGTGCGATTAAGCCAGACATGAAG
2	mEOS2 Rev	NotI	CTAGCGGCCGCTTTATCGTCTGGCATTGTCAGGCAATC
3	CD4(human) Fwd	EcoRI	TTCGAATTCTCGCCACCATGAACCGGGGAGTCCCTTTTAGG
4	CD4(human) Rev	BamHI	GGTGGATCCCGGGCAATGGGGCTACATGTCTTCTG

3.1.4 Enzymes

- restriction endonucleases (BamHI, NotI, EcoRI) and buffers
- FastAP Thermosensitive Alkaline Phosphatase, Taq polymerase, T4 ligase and buffers
  - *Fermentas, Burlington, Canada*
- Phusion High-Fidelity DNA polymerase, Phusion HF Buffer
  - *Thermo Scientific, Rockford, USA*

3.1.5 Chemical reagents

- DMSO, EDTA, ethidiumbromide, 1,4-dithio-D,L-threitol (DTT), glycine, Tween 20, kanamycin, ampicillin, iodacetamid, ammonium persulphate, polylysin
  - *Sigma-Aldrich, St. Louis, MO, USA*
- sodium chloride, sodium dihydrogen phosphate, disodium hydrogen phosphate, sodium diphosphate, potassium bicarbonate, hydrochloric acid, potassium acetate, ammonium chloride, paraformaldehyde, sucrose
  - *Lachner, Prague, CR*
- agarose, Tris, bromphenol blue
  - *Amresco, Solon, Ohio, USA*
- acetic acid, glycerol, isopropanol, methanol
  - *Penta, Prague, CR*
- loading dye for DNA electrophoresis, dNTPs
  - *Fermentas, Burlington, Canada*
- GeneRuler 1 kb and100 b DNA Ladder
  - *Thermo Scientific, Rockford, USA*
- Lipofectamin^{TM} 2000, Opti-MEM Reduced Serum Medium
  - *Invitrogen, Carlsbad, CA, USA*
- SDS, ethanol, HCl
  - *Merck, Darmstadt, Germany*
- 30% Acrylamide – Bis solution (29:1)
  - *Serva, Heidelberg, Germany*
- TEMED
  - *USB Corporation, Cleveland, USA*
- SDS-PAGE marker
  - *Bio-Rad Laboratories, Richmond, CA, USA*
- dried milk, low fat
  - *Promil, Novy Bydzov, CR*
- ECL Western blotting detection reagents
  - *Amersham Life Science Ltd., Little Chalfont, UK*

3.1.6 Buffers and solutions

- PBS (phosphate buffered saline)
  - 1.9 mM NaH_2PO_4, 8.1 mM Na_2HPO_4, 154 mM NaCl, pH 7.2
  - *prepared by tissue culture media facility IMG AS CR, Prague, CR*
- PBS-Tween
  - 1.9 mM NaH_2PO_4, 8.1 mM Na_2HPO_4, 154 mM NaCl, 0.05% Tween 20
  - *prepared by tissue culture media facility IMG AS CR, Prague, CR*
- TAE buffer
  - 40 mM Tris, 20mM acetic acid, 1 mM EDTA, pH 8
- sample buffer for SDS-PAGE (2X)
  - 100 mM Tris-HCl pH 6.8, 20% glycerol, 4% SDS, 0.02% bromphenol blue
- Tris-HCl buffer
  - 0.1 M Tris, 0.5M NaCl, pH 8
- SDS-PAGE Stacking gel solution
  - 3.6% acrylamide – bis solution (29:1), 0.125M Tris-HCl, 0.1% SDS, pH 6.8
- SDS-PAGE Separating gel solution
  - 8-10% acrylamide – bis solution (29:1), 0.375 M Tris-HCl, 0.1% SDS, pH 8.8
- SDS-PAGE running buffer
  - 250 mM glycine, 10 mM Tris, 0.1% SDS, pH 8.3
- Western blotting buffer
  - 48 mM Tris, 39 mM glycine, 20% methanol
- Lysis buffer
  - 20 mM Tris pH 7.5, 100 mM NaCl, 50 mM NaF, 10 mM $Na_4P_2O_7$, 10 mM EDTA, 5mM iodacetamide
- FACS buffer
  - PBS, 0.5% BSA, 0.1% NaN_3

3.1.7 Commercial DNA purification kits

- Zymoclean Gel DNA Recovery Kit, Zyppy Plasmid Miniprep Kit, DNA Clean & Concentrator Kit
  - *Zymo Research, Orange, USA*
- JETSTAR Plasmid Kit
  - *Genomed GmbH, Löhne, Germany*
- EndoFree Plasmid Maxi Kit
  - *QUIAGEN, GmBH, Hilden,Germany*

3.1.8 Antibodies

- MEM 241 – mouse monoclonal antibody against human CD4
  - *Home-made*
- GFP – rabbit polyclonal antibody against GFP protein
  - *Home-made*
- GAPDH – rabbit polyclonal antibody against human GAPDH protein
  - *Sigma, St. Louis, MO, USA*
- GAM M Px – goat anti mouse anti-IgM, conjugated with horse radish peroxidase
- GAR Px – goat anti rabbit, conjugated with horse radish peroxidase
  - *Bio-Rad Laboratories, Richmond, VA, USA*
- GAM A647 – goat anti mouse, conjugated with fluorescent dye AlexaFluor647
  - *Invitrogen, Carlsbad, CA, USA*
- GAM A647 – goat anti mouse, conjugated with fluorescent dye AlexaFluor647
  - *Invitrogen, Carlsbad, CA, USA*
- OKT3 – mouse IgG2a
  - *Home- made, prepared by Marek Cebecauer*

3.1.9 Laboratory devices

- pipettes and pipetmans
  - *Gilson, Middleton, USA*
- spectrophotometer Eppendorf BioPhotometer Plus, Eppendorf Thermomixer, centrifuges Eppendorf 5810R, 5417R, 5424
  - *Eppendorf, Hamburg, Germany*
- UV transluminator
  - *Herolab, Wiesloch, Germany*
- XP Cycler
  - *Bioer, Hangzhou, China*
- Ultrasonic Homogenizer - 4710 Series
  - *Cole-Parmer Instrument Co, Vernon Hills, IL, USA*
- Biorad Mini Protean III apparatus
  - *Bio-Rad Laboratories, Richmond, VA, USA*
- TE70X Semi-dry Transfer Unit, HE 33 Mini Submarine DNA elctrophoresis unit, PS 500XT DC power supply
  - *Hoefer Scientific Instruments, San Francisco, CA, USA*
- Fomei Optima developer
  - *Fomei, Hradec Kralove, CR*
- Leica TCS SP5 confocal microscope
  - *Leica Microsystems Heidelberg GmbH, Mannheim, Germany*
- Ecclipse TS100 microscope
  - *Nikon, Tokyo, Japan*
- Cellometer Auto T4
  - *Nexcelom Bioscience LLC, Lawrence, USA*
- Flow cytometer BDTM FACS Calibur
  - *BD Biosciences, San Jose, CA, USA*
- Vortex Genie 2
  - *Scientific Industries, New York, USA*
- Electrophoresis Power Supply
  - *Amersham pharmacia bitech, Uppsala, Sweden*
- ECM 830 square-wave electroporator
  - *Harvard Apparatus, Holliston, MA, USA*

- Neon® Transfection System
    - *Life technologies, Carlsbad, CA, USA*

3.1.10 Other material

- Microtubes 1.5 ml, PCR tubes 0,2 ml
    - *Eppendorf, Hamburg, Germany*
- tissue culture dishes and plates (6, 12, 24 wells), flasks (25cm^2 and 75cm^2), tubes 15 ml and 50 ml
    - *TPP, Trasadingen, Switzerland*
- BioTrace^{TM} NT Nitrocellulose Transfer Membrane
    - *Pall Corporation, New York, USA*
- Saran foil
    - *Dow Chemical, Midland, MI, USA*
- Kodak Medical X-ray General Purpose films, blue
    - *Kodak, Rochester, NY, USA*
- High precision coveslips
    - *Paul Marienfield GmBH, Landa-Kőnigshofen, Germany*
- ChamLide
    - *CMB, LCI, Seoul, Korea*
- Olympus IX71 with two TIRF modules, TIRFM objective Olympus UAPON100XOTIRF NA 1.49
    - *Life Sciences, Hamburg Germany*
- EMCCD camera
    - *Andor technology, Belfast, UK*
- Coherent
    - *Coherent, Santa Clara, CA, USA*

3.2 Methods

3.2.1 Polymerase chain reaction (PCR)

Polymerase chain reaction (PCR) enables amplification of desired DNA sequence using repeating cycles of DNA denaturation, sequence-specific primer annealing and DNA extension catalyzed by a thermostable DNA polymerase. The PCR reaction mixture contained Phusion High-Fidelity DNA polymerase (0.02u/µl; *Thermo Scientific*), Phusion HF Buffer (1X; *Thermo Scientific*), dNTPs mix (0.2mM of each nucleotide; *Fermentas*), forward and reverse primers (0.5µM; ordered from *Sigma-Aldrich*) and template DNA (10ng of plasmid DNA). The DNA denaturation was carried out at 98°C, 15s. The annealing temperature was designed according to the primers' sequence using Oligonucleotide Properties Calculator web site (http://www.basic.northwestern.edu/biotools/oligoalc.html) and annealing time 30s was used. DNA extension was performed at 72°C and the duration of this phase was designed according to the expected length of product considering extension rate 2-4 kb/min. The cycle was repeated 25 times. XP Cycler (*Bioer*) was used.

For direct screening of bacterial clones for the presence of an insert in a plasmid or when the correct orientation of an insert was examined, the bacterial colonies were picked from the agar plate used as DNA source for PCR. For this purpose, home-made Taq polymerase was used. The settings were the same as in the case of the Phusion polymerase, with exception of the DNA denaturation temperature which was 94°C. Extension rate 1kb/min was considered and 30 cycles were applied.

3.2.2 DNA electrophoresis in 1% agarose gel

DNA fragments are separated according to their length in agarose gel when voltage is applied. For the agarose gel preparation, 1% agarose and 0.5µg/ml ethidiumbromide were dissolved in 1X TAE buffer. Samples were mixed with 1/5 vol of loading dye (*Fermentas*), loaded into the gel and separated under constant voltage 100 V. DNA with intercalated ethidiumbromide were visualized using UV transluminator. The length of fragments in particular bands was assessed according to DNA marker GeneRuler 1 kb or 100b DNA Ladder (*Thermo Scientific*).

3.2.3 Isolation of DNA from agarose gel

Bands containing DNA fragments of desired size were cut out of the agarose gel and the DNA was isolated by Zymoclean Gel DNA Recovery Kit (*Zymo Research*).

3.2.4 DNA restriction cleavage

To cleave the plasmid DNA or PCR products in sequence specific manner, restriction endonucleases purchased from *Fermentas* were used. Reaction mixture included 2µg of plasmid DNA or estimated amount of PCR product, a restriction endonuclease (0.5u/µl; *Fermentas*) and appropriate restriction buffer recommended by manufacturer (*Fermentas*) were used. The digestion was carried out at 37°C for 2-4 hours or overnight.

3.2.5 Dephosphorylation of ends of digested plasmids

5'-end phosphates in the digested plasmids (vectors only) were removed before ligation with inserts to prevent their self-ligation. The cleaved plasmid DNA was treated with FastAP Thermosensitive Alkaline Phosphatase (*Fermentas*; 0.05u/µl, 37°C, and 20min). After incubation the phosphatase was deactivated by high temperature (75°C, 10min).

3.2.6 DNA ligation

To insert a DNA fragment to a linearized plasmid, DNA were mixed in molar ratio 10:1 (fragment:vector). The fragment was inserted into the plasmid due to the complementarity of DNA overhangs which were formed during the restriction cleavage. The DNA molecules were ligated by ligase enzyme. Quick Ligation Kit (*New England Biolabs*; 30min, RT or overnight, 16°C) or T4 ligase (*Fermentas*; 2 h, RT or overnight, 16°C) were used.

3.2.7 Bacterial transformation

Escherichia coli TOP10 strain of competent cells was used for transformation. Unfrozen bacteria were mixed with plasmid DNA (10ng) and incubated for 30min on ice. Afterwards, bacteria undergo heat shock (42°C, 45s) and were returned to the ice for

another 3 min. After addition of LB media (1ml), bacteria were incubated in Eppendorf Thermomixer (37°C, 30min, 800rpm). Bacteria were centrifugated (Eppendorf centrifuge 5417R, 10000g, 1min), resuspended in fresh LB media (100µl) and plated to LB agar plate supplied with ampicillin/kanamycin antibiotic serving for selection of the transformed clones carrying ampicillin/kanamycin resistance gene. Bacteria were grown overnight at 37°C.

3.2.8 "Single colony" DNA analysis

Escherichia coli TOP10 strain of competent cells was transformed with desired plasmid DNA according to the bacterial transformation protocol. One colony of all bacterial colonies grown overnight on selection plates was chosen for DNA isolation. Selected colony was picked up from agar plate and placed into appropriate volume of LB medium with ampicillin/kanamycin antibiotics added (100µg/l). Bacteria were grown overnight at 37°C.

3.2.9 Isolation of plasmid DNA

For minipreparative DNA isolation, transformed bacteria were grown in 3ml of LB medium with 100µg/l ampicillin/kanamycin and Zyppy Plasmid Miniprep Kit (*Zymo Research*) was used.

For midipreparative DNA isolation of plasmid DNA, bacteria were transformed according to bacterial transformation protocol and processed by "single colony" DNA analysis. Selected colonies were grown in 50ml of LB medium supplied with ampicillin (100µg/l). Plasmid DNA was isolated using JETSTAR Plasmid Kit (*Genomed*).

For large scale DNA isolation of plasmid DNA, bacteria were transformed according to bacterial transformation protocol and processed by "single colony" DNA analysis. Bacteria were grown in 100ml of LB medium supplied with ampicillin (100µg/l). Plasmid DNA was isolated using EndoFree Plasmid Maxi Kit (*Applied biosystems*).

3.2.10 DNA sequencing

Sequences of generated plasmids were checked by DNA sequencing. The plasmid DNA and appropriate primer chosen for sequencing were mixed according to the sequencing service instructions. Analysis of sequencing reaction products was performed by sequencing facility SEQme s.r.o. (http://www.seqme.eu).

3.2.11 Cell culture

Human cell line HEK293FT was cultured in DMEM medium, Jurkat T-cell line was cultured in RPMI 1640 medium, both supplied with 10% FBS (fetal bovine serum) and antibiotics (penicillin 100 U/ml, streptomycine 100 µg/ml, gentamicin 40 µg/ml). Cells were frozen in FBS supplied with 10% DMSO (*Sigma-Aldrich*) and stored in liquid nitrogen.

3.2.12 Cell transfection

Cell transfection methods enable introduction of plasmids coding specific protein products into cells. Lipofection and two electroporation techniques to transfect cells with vectors carrying DNA constructs were used.

3.2.12.1 Lipofection

Lipofection is a transfection technique that enables introduction of a particular DNA sequence to cells and transient expression of recombinant proteins. Positively charged lipids are used as the transfection vehicles. They create complexes with negatively charged DNA molecules and, thereby, enable their passage through the lipophilic plasma membrane. As the lipofection reagent, Lipofectamin^{TM} 2000 (*Invitrogen*) was used. HEK 293FT cells were tranfected by lipofection.

Plasmid DNA was diluted in Opti-MEM Reduced Serum Medium (*Invitrogen*; Opti-MEM) to final concentration 16ng/µl. In another tube, Lipofectamin^{TM} 2000 was mixed with Opti-MEM in ratio 1:25 and incubated for 5min at RT. After 5min incubation, diluted DNA was combined with the Lipofectamin^{TM} 2000 solution and coincubated together (20min, RT).

The mixture was then dropped on a culture of cells grown in antibiotic-free DMEM medium and incubated at 37°C for 24hours.

3.2.12.2 Electroporation

Electroporation technique is cell transfection technique suitable especially for suspension cells. Jurkat T cells were electroporated. 10^7 cells were used for single electroporation.

Appropriate volume of RPMI medium supplied with 10% FBS was warmed up in advance. Cells were washed with RPMI without antibiotics or FBS. Appropriate number of washed cells was applied to 4mm gap cuvettes (in 300ul RPMI/ 10^7 cells). 10ug of DNA was added to the cell suspension, no vortex was used for mixing (only "finger tap" technique). The mixture in cuvettes was incubated for 10-15min at room temperature in the hood. Cells were electroporated using ECM 830 square-wave electroporator (voltage 300V, pulse length 10ms, mode LV, and pulse 1). Electroporated cells were transferred immediately to pre-heated RPMI medium with 10% FCS without antibiotics. Cells were grown for 36hours in the incubator (5%CO2, 37°C).

3.2.12.3 Microporation

Microporation is a variant of electroporation technique suitable especially for difficult transfections. Here, Jurkat cells were electroporated. PBS washed cells were resuspended in R buffer (10^7 cells per one electroporation). 1ug DNA per one shot was added to cell suspension, one shot corresponds to 10ul of cell suspension in R buffer. Cells were electroporated in tip with golden electrode according to the manufacturer's recommendations.

3.2.13 Preparation of cell lysates for SDS-PAGE

Cells were resuspended in PBS and then lyzed with the same volume of 2X sample buffer. Samples were sonicated by Ultrasonic Homogenizer – 4710 Series (50 % of amplitude, 15s) to fragment cellular DNA. Next, samples were boiled in Eppendorf Thermomixer (96°C, 2min), dithiothreitol was added (final concentration 1 %) to reduce

proteins and samples were boiled once again (96°C, 1min). Lysates were loaded onto polyacrylamide gel.

3.2.14 SDS-PAGE

Migration of proteins through the porous polyacrylamide gel in presence of sodium dodecyl sulphate (SDS) which is driven by constant voltage causes their separation according to their molecular weight (MW). SDS is an anionic detergent with amphiphilic character that covers proteins evenly using its hydrophilic part and confers negative charge on them using its anionic part enabling the separation in electric field.

Concentration of the separation gel was 8 % (according to MW of detected protein), concentration of the stacking gel was 3.6 %. The length of the gels was approximately 5 and 1.5cm, respectively. Electrophoresis was carried out using Biorad Mini Protean III apparatus under constant voltage of 120V.

3.2.15 Western blotting

Proteins separated by SDS-PAGE were transferred from the polyacrylamide gel to BioTrace^{TM} NT Nitrocellulose Transfer Membrane (*Pall Corporation*) by TE70X Semi-dry Transfer Unit (*Hoefer*). The transfer was carried out under constant electric current 0.8mA/cm^2 (of the membrane) for 75 min. Before the transfer, the gel, the nitrocellulose membrane and chromatographic paper were washed in blotting buffer.

3.2.16 Detection of proteins using specific antibodies

The nitrocellulose membrane with immobilized proteins was blocked with 5% milk (*Promil)* in PBS-Tween buffer for 30 min that ensures saturation of protein-binding capacity of the membrane and thereby prevents non-specific binding of antibody. The membrane was subsequentially incubated with primary antibody (usually 1000X diluted in1% milk in PBS-Tween) against an epitope in a detected protein. The membrane was incubated 0.5-12 hours depending on expected amount of protein to be detected. The membrane was washed with PBS-Tween three times during 30min. Washed membrane was than incubated with secondary antibody conjugated with horse radish peroxidase enzyme (10000X diluted in 1% milk in PBS-Tween, 30 min). The membrane was washed

with PBS-Tween three times during 30min. To visualize a detected protein, enzymatic activity of the horse peroxidase conjugated to the secondary antibody was exploited. The membrane was incubated with ECL Western blotting detection reagents for 80 s (*Amersham Life Science Ltd.*). The chemoluminiscence reaction was detected by exposure to X-ray film (Kodak Medical X-ray General Purpose, blue; *Kodak*) and developer device Fomei Optima (*Fomei*).

3.2.17 Confocal microscopy – live cell imaging

Confocal microscope Leica TCS SP5 was used to examine membrane localization of generated fusion proteins. Cells were electroporated using microelectroporation protocol. Immediately before examining cells under the microscope, they were centrifugated (Eppendorf centrifuge 5810R, 450g, 4min) and resuspended in PBS. Resuspended cells were added to polylysin covered coverslip placed in ChamLide device and incubated for 3min to immobilize cells. Colorless RPMI medium supplied with 10%FCS was added to cells after incubation to prevent cell death over the period of imaging.

3.2.18 Polylysin coated coverslips

High precision coverslips were 5x washed with distilled water. 0.1% polylysin in H_2O was added to dry coverslips and incubated for 1 hour at room temperature. Polylysin suspension was removed and the coverslips were dried spontaneously at room temperature.

3.2.19 Preparation of cell samples for FACS analysis

For fluorescent protein fusion proteins (EGFP constructs) detection, cells were resuspended in FACS solution and analyzed immediately.

For measurement of the expression of cell surface markers, cells were stained with a fluorophore-conjugated antibody against a particular antigen. The staining was carried out on ice. Cells were resuspended in FACS solution and incubated with primary anti human CD4 antibody MEM241 for 20 min (1:100). Stained cells were washed twice with FACS solution and incubated with secondary antibody conjugated with fluorophore AlexaFluor647 for 20min. After incubation, cells were washed twice in FACS solution and analyzed.

3.2.20 Fluorescence-activated cell sorting (FACS)

FACS analysis is a high-speed fluorescence-based method enabling measurement of fluorescence of single cells in addition to characterization of their size and complexity and cell counting. Thus, for instance, fluorescent antibody-stained cell surface markers and intracellular molecules or fluorescent proteins expressed by cells can be detected. In our experiments, FACS analysis was used to detect cell surface markers, expression of fusion proteins containing a fluorescent protein. For these purposes, Flow cytometer BDTM FACS Calibur in Flow Cytometry and Light Microscopy core facility at IMG AS CR was used. FlowJo (*Tree Star, Oregon, USA*) software was used to analyze FACS data.

3.2.21 Preparation of samples for single molecule microscopy

For imaging of activated T cells, transfected Jurkat T cells were stimulated by incubation on OKT3 antibody coated coverslips and fixed according to the protocol.

3.2.21.1 Jurkat cell activation

Coverslips were incubated (coated) with 20µg/ml antibody solution (OKT3) in PBS for 1 hour, 37ºC. Remaining surface was blocked with addition of complete RPMI medium (supplied with 10% FBS) for 15min, 37ºC. Medium was removed, coverslips were washed with PBS. 250ul of transfected Jurkat T cells in colorless medium were added to coverslips for activation. Cells were activated for appropriate time at 37ºC and fixed immediately.

3.2.21.2 Cell fixation

Jurkat T cells, transfected according to the protocol, were fixed by adding of 4% PFA (paraformaldehyde) with 2% Sucrose in PBS for 8 minutes at 37ºC. Fixation solution was removed and cells were washed two times with 0,1M NH_4Cl in PBS for 5 minutes and thereafter twice with PBS and stored at 4ºC before imaging (within 2-3 days).

3.2.22 PALM data acquisition and analysis

Superresolution analysis of transfected Jurkat T cells was provided using home-made single molecule TIRF microscope with Olympus IX71 body equipped with NA1.49 TIRFM objective Olympus UAPON100XOTIRF and diode lasers 405, 488, 561 and 643 nm (150 mW; *Coherent*) coupled to TIRF module. Data were acquired on highly-sensitive EM-CCD camera (*Andor technology*) using home-made acquisition control software based on LabView (thanks to Ales Benda, JHI AS CR, Prague). Acquisition settings: 30ms/frame; 256x256 pixels, 10-20.000 frames collected, EM mode: 300. Data were first processed by ImageJ/FiJi (Schindelin et al., 2012) to manually eliminate frames with no or poor signal. Localization of single molecule fluorescence events was performed using rapidSTORM software (Wolter et al., 2010). Localization data were further processed using MATLAB scripts from Dave Williamson and Katharina Gaus (University of New South Wales, Sydney) for cluster analysis (Owen et al., 2012).

4 Results

4.1 Generation of DNA constructs

4.1.1 Human CD4 glycoprotein and its variants

CD4 wt and its mutated forms (Tab. 1; see Fig. 3 in Introduction) were kind gift from laboratories of Waldemar Popik (W.P., Meharry Medical College, Nashville, U.S.) and Stèphane Basmaciogullari (S.B., Institute Necker, Paris, France). Plasmids from W.P. already encode EGFP fusion CD4 variants, those from S.B. contain only CD4 sequences. For further characterization of constructs it was necessary to prepare missing variants with EGFP and mEOS2. Fusion with EGFP fluorescent protein enables investigation of constructs by confocal microscopy whereas fusion proteins with mEOS2 were required for localization microscopy.

CD4 variant	origin	vector	mutation
CD4 wt1 EGFP	W.P.	pEGFP-N1	none
CD4 CS1 EGFP	W.P.	pEGFP-N1	C419,C422 -› S419,S422 (CS1)
CD4 RA5 EGFP	W.P.	pEGFP-N1	RXRRR -› AAAAA (RA5)
CD4 CS1 RA5 EGFP	W.P.	pEGFP-N1	CS1 + RA5
CD4 wt2	S.B.	pCG	none
CD4 CS2	S.B.	pCG	C445,C447 -› S445,S447 (CS1)

Tab.1 CD4 constructs used in this work.

5’…CTC**GAGCTC**AAGCTTC**GAATTC**TCGCCACCATGAACCGGGGAGTCCCTTTTAGGCACT
TGCTTCTGGTGCTGCAACTGGCGCTCCTCCCAGCAGCCACTCAGGGAAAGAAAGTGGTGCTGGG
CAAAAAAGGGGATACAGTGGAACTGACCTGTACAGCTTCCCAGAAGAAGAGCATACAATTCCA
CTGGAAAAACTCCAACCAGATAAAGATTCTGGGAAATCAGGGCTCCTTCTTAACTAAAGGTCCA
TCCAAGCTGAATGATCGCGCTGACTCAAGAAGAAGCCTTTGGGACCAAGGAAACTTTCCCCTGA
TCATCAAGAATCTTAAGATAGAAGACTCAGATACTTACATCTGTGAAGTGGAGGACCAGAAGG
AGGAGGTGCAATTGCTAGTGTTCGGATTGACTGCCAACTCTGACACCCACCTGCTTCAGGGGCA
GAGCCTGACCCTGACCTTGGAGAGCCCCCCTGGTAGTAGCCCCTCAGTGCAATGTAGGAGTCCA
AGGGGTAAAAACATACAGGGGGGGAAGACCCTCTCCGTGTCTCAGCTGGAGCTCCAGGATAGT
GGCACCTGGACATGCACTGTCTTGCAGAACCAGAAGAAGGTGGAGTTCAAAATAGACATCGTG
GTGCTAGCTTTCCAGAAGGCCTCCAGCATAGTCTATAAGAAAGAGGGGGAACAGGTGGAGTTC
TCCTTCCCACTCGCCTTTACAGTTGAAAAGCTGACGGGCAGTGGCGAGCTGTGGTGGCAGGCGG
AGAGGGCTTCCTCCTCCAAGTCTTGGATCACCTTTGACCTGAAGAACAAGGAAGTGTCTGTAAA
ACGGGTTACCCAGGACCCTAAGCTCCAGATGGGCAAGAAGCTCCCGCTCCACCTCACCCTGCCC
CAGGCCTTGCCTCAGTATGCTGGCTCTGGAAACCTCACCCTGGCCCTTGAAGCGAAAACAGGAA
AGTTGCATCAGGAAGTGAACCTGGTGGTGATGAGAGCCACTCAGCTCCAGAAAAATTTGACCT
GTGAGGTGTGGGGACCCACCTCCCCTAAGCTGATGCTGAGTTTGAAACTGGAGAACAAGGAGG
CAAAGGTCTCGAAGCGGGAGAAGGCGGTGTGGGTGCTGAACCCTGAGGCGGGGATGTGGCAGT
GTCTGCTGAGTGACTCGGGACAGGTCCTGCTGGAATCCAACATCAAGGTTCTGCCCACATGGTC
CACCCCGGTGCAGCCAATGGCCCTGATTGTGCTGGGGGGCGTCGCCGGCCTCCTGCTTTTCATT
GGGCTAGGCATCTTCTTCTGTGTCAGGTGCCGGCACCGAAGGCGCCAAGCAGAGCGGATGTCTC
AGATCAAGAGACTCCTCAGTGAGAAGAAGACCTGCCAGTGTCCTCACCGGTTTCAGAAGACAT
GTAGCCCCATTGCCCG**GGATCC**ACCGGTCGCCACCATGGTGAGCAAGGGCGAGGAGCTGTTCA
CCGGGGTGGTGCCCATCCTGGTCGAGCTGGACGGCGACGTAAACGGCCACAAGTTCAGCGTGT
CCGGCGAGGGCGAGGGCGATGCCACCTACGGCAAGCTGACCCTGAAGTTCATCTGCACCACCG
GCAAGCTGCCCGTGCCCTGGCCCACCCTCGTGACCACCCTGACCTACGGCGTGCAGTGCTTCAG
CCGCTACCCCGACCACATGAAGCAGCACGACTTCTTCAAGTCCGCCATGCCCGAAGGCTACGTC
CAGGAGCGCACCATCTTCTTCAAGGACGACGGCAACTACAAGACCCGCGCCGAGGTGAAGTTC
GAGGGCGACACCCTGGTGAACCGCATCGAGCTGAAGGGCATCGACTTCAAGGAGGACGGCAAC
ATCCTGGGGCACAAGCTGGAGTACAACTACAACAGCCACAACGTCTATATCATGGCCGACAAG
CAGAAGAACGGCATCAAGGTGAACTTCAAGATCCGCCACAACATCGAGGACGGCAGCGTGCAG
CTCGCCGACCACTACCAGCAGAACACCCCCATCGGCGACGGCCCCGTGCTGCTGCCCGACAACC
ACTACCTGAGCACCCAGTCCGCCCTGAGCAAAGACCCCAACGAGAAGCGCGATCACATGGTCC
TGCTGGAGTTCGTGACCGCCGCCGGGATCACTCTCGGCATGGACGAGCTGTACAAGTAA**AGCG**
GCCGCGACTCTAGA… 3’

Fig. 7 Sequence of human CD4 glycoprotein (in yellow), including sequence of spacer (in blue), sequence of EGFP fluorescent protein (in green) and restriction sites in bold.

4.1.2 Human CD4 gene fused to EGFP (W. P.)

CD4-EGFP plasmids received from W.P. were amplified in *E. coli* bacterial strain Top10 and processed by "single colony" DNA analysis. The plasmid DNA was isolated from the cell culture by minipreparative DNA isolation method. Verification of the presence of CD4-EGFP constructs in the plasmid was performed using restriction with endonucleases *EcoRI* and *NotI*. The result of restriction was then analyzed by 1% agarose gel electrophoresis (Fig. 8).

4.1.3 Generation of mEOS2 fluorescent variants from CD4 EGFP var. (W. P.)

Fluorescent protein EGFP in original CD4-EGFP sequences was replaced by photoconvertible fluorescent protein mEOS2. mEOS2 used in cloning was generated by PCR using primers in Tab. 2 according to Phusion polymerase PCR protocol from pRSLAT-mEOS2 template DNA (obtained from K. Gaus, University of New South Wales, Sydney, Australia). Presence of PCR product of expected size 681bp was analyzed by 1% DNA agarose gel electrophoresis (Fig. 9). DNA was purified from agarose gel using Zymoclean™ DNA gel recovery kit. 5' and 3' ends of mEOS2 sequence were prepared for sticky-end ligation using restriction enzymes *BamHI* and *NotI*.

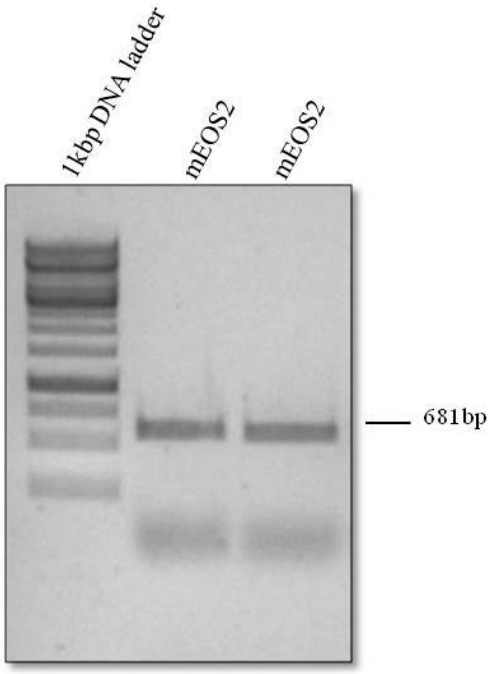

Fig. 8 Control digestion of CD4-EGFP W.P. variants.

CD4-EGFP W.P. constructs were digested sequentially by endonucleases *EcoRI* and *NotI* to verify the presence of sequences in original pEGFP-N1 vector and to verify the proper sizes. Products of size 3961bp correspond to empty vectors pEGFP-N1, whereas those with size of 2134bp correspond to CD4-EGFP insert.

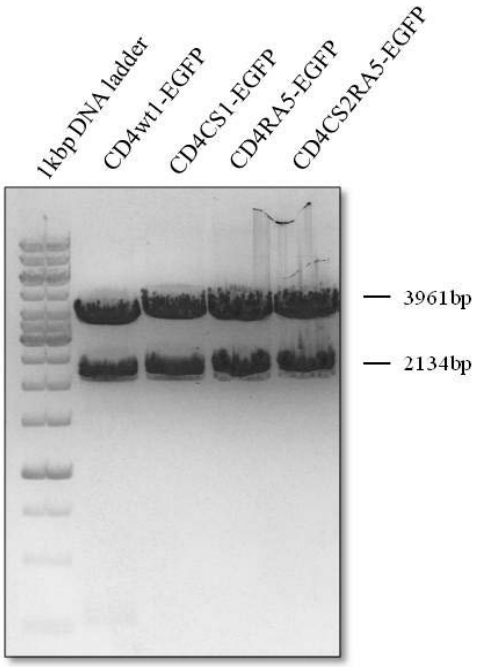

Fig. 9 mEOS2 sequence acquired in PCR reaction.
Sequence of mEOS2 was acquired from pRSLAT-mEOS2 template DNA in PCR according to standard phusion polymerase protocol using primers in Tab. 2. Products in size of 681bp correspond to a sequence of mEOS2 PCR product

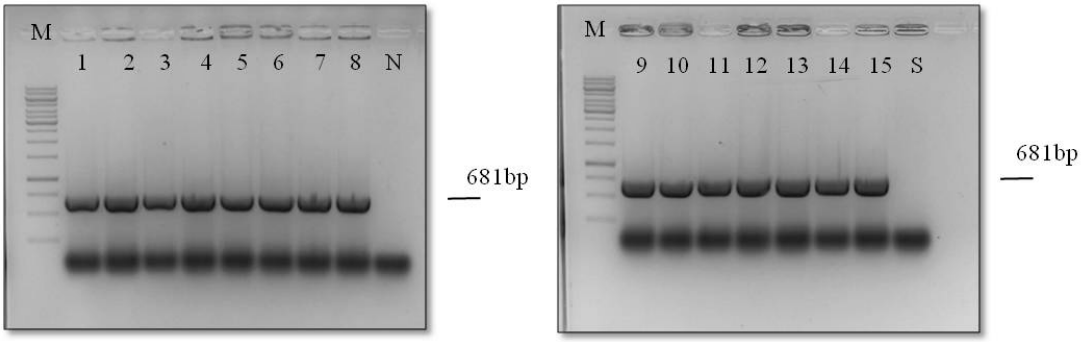

Fig. 10 Colonies screened for ligation of CD4wt1-mEOS2 construct.
Selected bacterial colonies from CD4wt1-mEOS2 ligation were screened using PCR reaction for the presence of mEOS2 sequence as an evidence of successful ligation.
1-15 - bacterial colonies used for PCR screening to generate mEOS2
N - negative control lacking bacterial DNA, S - colony from self-ligation of vector pEGFP-N1
M - 1kbp DNA ladder

Fwd BamHI	5´GAA**GGATCC**ACCGGTCGCCACCATGAGTGCGATTAAGCCAGACATGAAG 3´
Rev NotI	5´CTA**GCGGCCGC**TTTATCGTCTGGCATTGTCAGGCAATC 3´

Tab. 2 Primers designed for mEOS2 PCR with highlighted restriction sites (bold).

Original plasmid containing CD4wt1-EGFP was prepared for replacement of EGFP coding sequence by digestion using the same restriction enzymes (*BamHI* and *NotI*). Both restrictions were separated by 1% agarose gel electrophoresis. Linearized plasmid containing CD4wt but no EGFP sequence and digested insert mEOS2 were isolated from the gel using Zymogene^{TM} gel recovery kit. Vector and insert DNA were ligated using T4 DNA ligase. Ligation mixture was than transformed to competent bacteria and plated on agar plates with kanamycin antibiotic selection. Colonies were observed on agar plate with CD4wt1-mEOS2 ligation and not on selfligation control (empty pEGFP-N1 vector) with exception of single colony.

Bacterial colonies grown for CD4wt1-mEOS2 and for selfligaton control were screened for desired ligation product by PCR reaction using primers in Tab. 2 according to Taq polymerase screening colonies protocol (Fig. 10). All bacterial colonies from plate with pCD4wt1-mEOS2 ligation were suitable for further processing. Correctly, no product was observed from a colony selected from plate with selfligation control. One colony from plate with pCD4wt1-mEOS2 ligation was selected, amplified and DNA was isolated using midipreparative DNA isolation method. The mEOS2 from CD4wt1-mEOS2 construct was further used for subcloning of the remaining three versions of CD4 constructs.

Plasmids pCD4CS1-EGFP, pCD4RA5-EGFP and pCD4CS1RA5-EGFP were digested using restriction enzymes *NotI* and *BamHI* to remove EGFP sequence. pCD4wt1-mEOS2 plasmid was also digested with *NotI* and *BamHI* enzymes to release mEOS2 sequence. mEOS2 sequence was ligated by T4 DNA ligase to linearized pCD4CS1, pCD4RA5 and pCD4CS1RA5 plasmids. Ligation mixture was transformed into competent bacteria and DNA was isolated by minipreparative isolation method. All newly generated CD4-mEOS2 constructs were subsequently analyzed by *BamHI* and *NotI* restriction (Fig. 11). All CD4-EGFP and CD4-mEOS2 constructs were amplified in bacteria and plasmid DNA was isolated and purified using Large-scale DNA isolation kit for high yield of very clean DNA (Tab. 3).

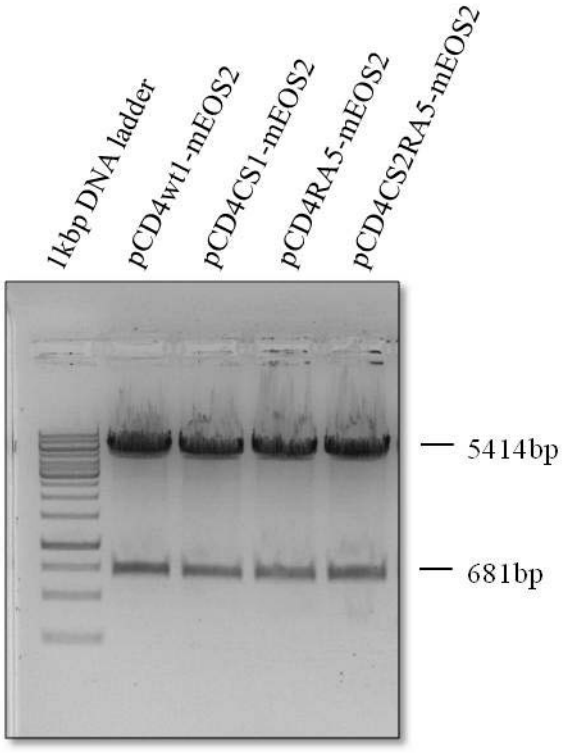

Fig. 11 Double restriction analysis of CD4-mEOS2 constructs.

Generated CD4-mEOS2 constructs were digested by endonucleases *BamHI* and *NotI* to verify successful ligation of mEOS2 sequence into CD4 constructs. Products in size of 5414bp correspond to CD4 containing vectors. Products in size of 681bp correspond to a sequence of mEOS2.

Plasmid	Concentration [µg/ml]	Absorbance ratio 260/280
pCD4wt1-EGFP	4710	1,76
pCD4CS1-EGFP	4318	1,73
pCD4RA5-EGFP	4288	1,74
pCD4CS1RA5-EGFP	3613	1,73
pCD4wt2-EGFP	1330	1,75
pCD4CS2-EGFP	1010	1,74
pCD4wt1-mEOS2	2330	1,80
pCD4CS1-mEOS2	2000	1,80
pCD4RA5-mEOS2	1857	1,78
pCD4CS1RA5-mEOS2	2345	1,78
pCD4wt2-mEOS2	1350	1,76
pCD4CS2-mEOS2	1100	1,74

Tab. 3 Generated CD4 fusion constructs, quantities of DNA and its purity.

Plasmid DNA concentration was measured using Eppendorf® BioPhotometer spectrophotometer. The ratio of absorbance at 260 nm and 280 nm is used to estimate the purity of DNA. A ratio of ~1.8 is generally accepted as “pure” for DNA. If the ratio is appreciably lower, it may indicate the presence of protein or other contaminants that absorb strongly at or near 280 nm.

CD4 (human)	Fwd EcoRI	5´TTC**GAATTC**TCGCCACCATGAACCGGGGAGTCCCTTTTAGG 3´
CD4 (human)	Rev BamHI	5´GGT**GGATCC**CGGGCAATGGGGCTACATGTCTTCTG 3´
mEOS2	Rev NotI	5´CTA**GCGGCCGC**TTTATCGTCTGGCATTGTCAGGCAATC 3´

Tab. 4 Primers used for sequencing of CD4 construct with highlighted restriction sites (bold).

All generated constructs were sequenced using primers in Table 4. Sequencing revealed no discrepancies.

4.1.4 Human CD4 genes in pCG vector (S.B.)

CD4 constructs obtained from S.B. in pCG vector lacked fusion with any fluorescent protein. For further use it was important to isolate CD4 sequences from pCG vectors and subclone into previously generated plasmids containing EGFP and mEOS2 sequences.

pCG plasmids encoding CD4 variants from S.B. were amplified in *E. coli* bacterial strain TOP10 and processed by "single colony" DNA analysis method. The plasmid DNA was isolated from the bacterial culture by minipreparative DNA isolation method. Verification of the presence of CD4 constructs in the obtained plasmids was performed using restriction with endonucleases *XbaI* and *BamHI*. The result of restriction was then analyzed by 1% DNA agarose gel electrophoresis (Fig. 12). pCG-CD4 plasmids were used as template DNA for PCR reaction using primers in Tab. 5 according to Phusion polymerase PCR protocol. Appropriate restriction sites for sticky-end ligation were inserted with primers during PCR reaction.

Fwd EcoRI	5' TTC**GAATTC**TCGCCACCATGAACCGGGGAGTCCCTTTTAGG 3'
Rev BamHI	5' GGT**GGATCC**CGGGCAATGGGGCTACATGTCTTCTG 3'

Tab. 5 Primers designed for CD4 (S.B.) PCR with highlighted restriction sites (bold).

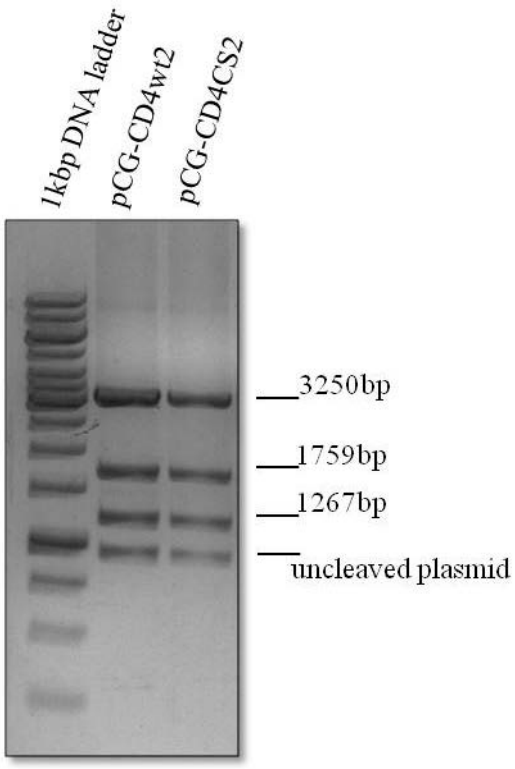

Fig. 12 Control digestion of CD4 S.B. variants. pCG-CD4 S.B. constructs were digested by endonucleases *XbaI* and *BamHI* to verify the presence of CD4 sequences in original pCG vectors. Product in size of 3250bp, 1759bp and product in size of 1267bp corresponds to digested pCG-CD4 plasmid in original size of 6276bp. An additional band is most probably contamination of uncleaved plasmid.

PCR product was analyzed by 1% agarose gel electrophoresis (Fig. 13A). CD4 DNA was purified from agarose gel using Zymoclean™ DNA gel recovery kit and modified by restriction with enzymes *BamHI* and *EcoRI*. Similarly vectors pCD4wt1-EGFP and pCD4wt1-mEOS2 were processed using the same enzymes. Digested sequences from all restrictions were separated on the 1% agarose gel (Fig. 13B) and DNA was purified using Zymoclean™ DNA gel recovery kit. CD4wt2 and CD4CS2 sequences isolated from pCG plasmids were ligated to linearized p-EGFP or p-mEOS2 vectors by T4 DNA ligase. Ligation mixtures were transformed to competent bacteria and amplified. DNA was isolated by minipreparative DNA isolation method and digested with restriction enzymes *BamHI* and *EcoRI* to perform control analysis (Fig. 14).

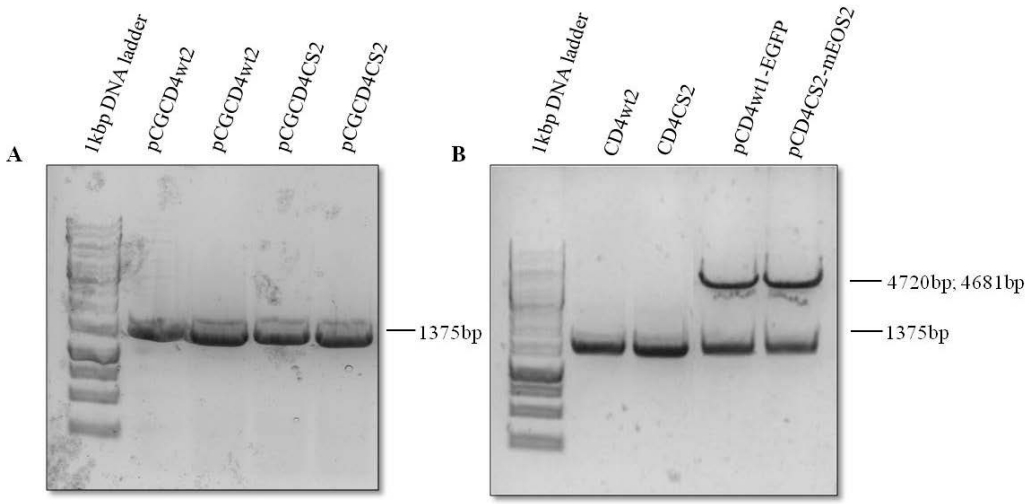

Fig. 13 Processing of CD4 S.B. constructs and pCD4wt1-EGFP or pCD4wt1-mEOS2 before ligation.

A. Sequences of CD4wt2 and CD4CS2 were acquired in PCR reaction of pCG-CD4wt2/CS2 template using primers in Tab. 4. Size of PCR products was 1375bp.

B. CD4wt1 sequence from pCD4wt1-EGFP and pCD4wt1-mEOS2 vectors was removed using *BamHI* and *EcoRI* endonucleases. Sequence of vector-EGFP without CD4 corresponds to 4720bp, sequence of linearized vector-mEOS2 corresponds to 4681bp. Sequence of digested CD4 corresponds to 1375bp.

PCR products CD4wt2 and CD4CS2 digested with *BamHI* and *EcoRI* endonucleases were ligated to replace CD4wt1 sequence in both acceptor vectors.

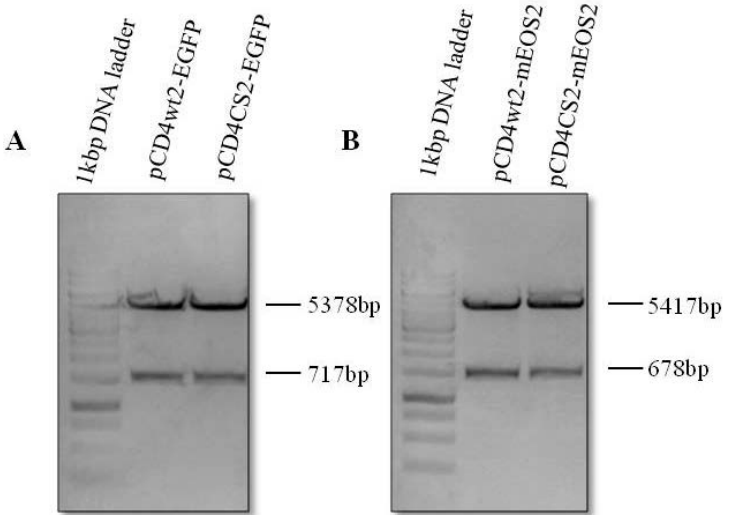

Fig.14 Restriction analysis of pCD4wt2/CS2 plasmids.

A. Digestion of pCD4wt2-EGFP and pCD4CS2-EGFP plasmids using *BamHI* and *EcoRI* endonucleases. Products in size of 5378bp correspond to plasmids with CD4wt2 or CD4CS2. Products in size of 717bp correspond to EGFP sequence.

B. Digestion of pCD4wt2-mEOS2 and pCD4CS2-mEOS2 plasmids using *BamHI* and *EcoRI* endonucleases. Products in size of 5417bp correspond to plasmids with CD4wt2 or CD4CS2. Products in size of 678bp correspond to mEOS2 sequence.

Selected clones of pCD4wt2-EGFP, pCD4CS2-EGFP, CD4wt2-mEOS2 and CD4CS2-mEOS2 were amplified in bacteria. DNA was isolated using large scale DNA isolation kit for high yield of very clean DNA (Tab. 3).

All generated constructs were sequenced using primers in Table 4. Sequencing revealed no discrepancies.

Note that sequencing of generated CD4 constructs ascertained the uniformity of CD4wt1 and CD4wt2 sequences.

4.2 Characterization of CD4 protein expression

4.2.1 Western blotting and immunodetection in HEK293FT cells

The capacity of generated constructs to express the appropriate fluorescent fusion proteins in mammalian cells was first studied at protein level. HEK293FT cell line allows easy transfection and high protein yield and was, therefore, selected for biochemical analysis of recombinant proteins by Western blot method.

HEK293FT cell line was transfected by Lipofectamine®2000 method using previously generated CD4 constructs (Tab. 3). Cell lysates were prepared after growing cells for 24 hours at 37ºC in 5% CO_2 atmosphere. Presence of CD4 protein variants and fusion to EGFP was tested by immunoblotting employing antibodies with specify to both parts of fusion proteins. Antibodies against human CD4 and GFP were used (Fig. 15; Fig. 16), respectively. Cell lysates were separated using SDS-PAGE method, transferred to nitrocellulose membrane and after staining with appropriate antibodies detected using Western Lightning® Chemiluminescence Reagent Plus system.

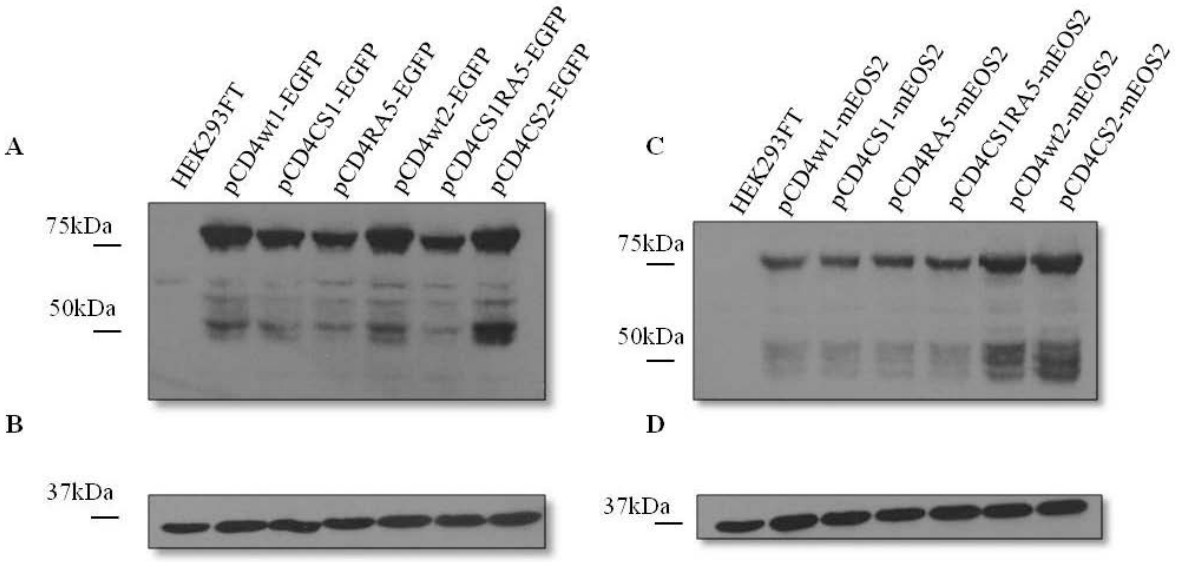

Fig. 15 CD4 plasmid variants transfected in HEK293FT cells line and detected for the presence of human CD4.

A. CD4-EGFP and **C.** CD4-mEOS2 fusion variants analyzed by immunoblotting with specific antibody detecting human CD4 glycoprotein (MEM241).

B. and **D.** Transfected HEK293FT cells analyzed by immunoblotting with antibody specific for GAPDH used to verify uniform loading of samples.

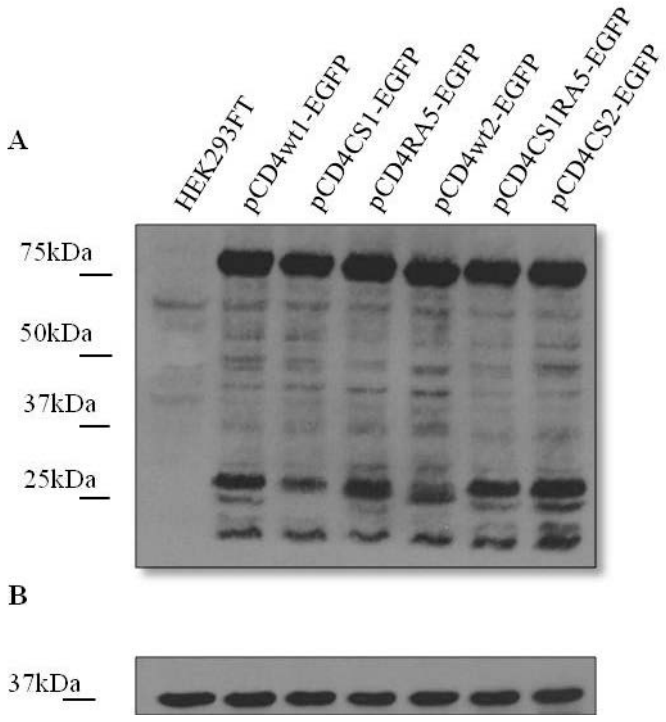

Fig. 16 CD4-EGFP fusion variants transfected in HEK293FT cell line and detected for the expression of GFP.

A. CD4-EGFP fusion variants analyzed by immunoblotting with specific antibody detecting GFP.

B. Transfected HEK293FT cells analyzed by immunoblotting with antibody specific for GAPDH used to verify uniform loading of samples.

Expected molecular weight of CD4-EGFP construct was about 78kDa and expected molecular weight of CD4-mEOS2 was about 77kDa. The observed data proved the evidence of CD4-EGFP and CD4-mEOS2 expression with the correct molecular weight. CD4-mEOS2 protein constructs were not tested using specific mEOS2 antibody due to a lack of appropriate antibody in the laboratory. Origin of mEOS2 photoconvertible protein differs from that of GFP. It was decided to prove the correct expression and folding of CD4-mEOS2 protein variants by localization microscopy method in view of the fact that correctly folded protein would enable the photoconversion after exposure to the UV light.

An interesting phenomenon can be observed here. Misfolded CD4 fusion proteins decompose to fluorescent protein (EGFP) and CD4 glycoprotein. The bands with molecular weight of 51kDa correspond to the correct size of CD4 glycoprotein lacking fusion to fluorescent protein (Fig. 15). The bands corresponding to the molecular weight of 26kDa are probably misfolded EGFP parts which separated from CD4 glycoprotein (Fig. 16). This event is further discussed in the chapter “Discussion” further in the text.

4.2.2 Flow cytometry in Jurkat T cell line

Our primary interest is to investigate behavior of CD4 in human cells. Therefore, we decided to further investigate CD4 glycoprotein expression in living T cells. Jurkat T cells (cell line derived from T-cell lymfoblastoma) is the most common human T cell line available in our laboratory and was selected for further characterization of generated constructs. It was decided to examine the expression of CD4 plasmid variants on the surface of Jurkat T cell line using fluorescence-activated cell sorting (FACS) method and confocal microscopy. First Jurkat cells were electroporated according to the standard electroporation protocol using pCD4wt1-EGFP plasmid and then treated with mouse primary anti-human CD4 antibody (MEM241), and subsequently, with fluorescent goat anti-mouse Ig AlexaFluor647 secondary antibody (Fig. 17).

It was intended to draw a comparison between expression of endogenous CD4 glycoprotein and increased CD4 expression due to electroporation with CD4wt1-EGFP plasmid. The increase of surface CD4 glycoprotein expression in electroporated Jurkat cells in comparison with untransfected sample was marginal (Fig. 17A). GFP fluorescence intensity measurement of pCD4wt1-EGFP electroporated Jurkat cells in comparison to nonfluorescent negative control indicated low expression of exogenous CD4 surface glycoprotein (Fig. 17B).

Poor transfection efficiency combined with minor increase in CD4 expression levels was unconvincing. Therefore, it was decided to further examine the expression of CD4 fusion plasmids in Jurkat cells using live cell imaging and different transfection technique.

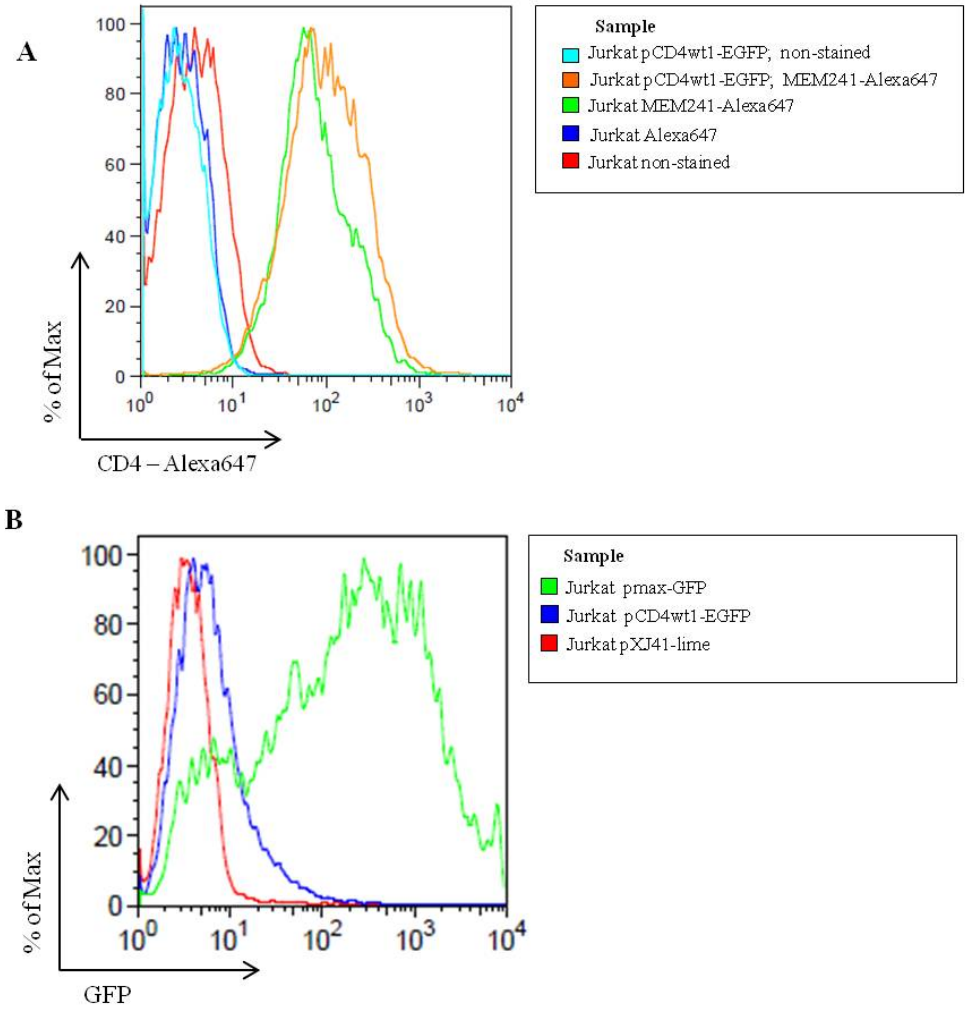

Fig. 17 Flow cytometry analysis of CD4 expression in Jurkat cells transfected with pCD4wt1-EGFP plasmid.

A. Flow cytometry of Jurkat cells unstained (red), stained only with secondary antibody (dark blue), Jurkat cells electroporated with pCD4wt1-EGFP unstained (orange) and stained with anti-CD4 primary antibody (MEM241) and AlexaFluor647 conjugated secondary antibody (light blue).

B. Histogram comparing EGFP expression of different plasmids. Jurkat cells electroporated with non-fluorescent plasmid pXJ41-Lime used as negative control are shown in red, pmax-GFP fluorescent protein as positive control in green and with pCD4wt1-EGFP in blue.

4.2.3 Confocal microscopy in Jurkat T cells

The next step was the examination of protein expression level as well as its localization in transfected cells using confocal microscopy.

Here, Jurkat cells were electroporated using a different variant of electroporation, microporation technique using NEON transfection tool and a set of CD4 constructs contained in Tab. 3. Transfected cells were immobilized on polylysin coated coverslips for imaging.

Data achieved by confocal microscopy using EGFP fusion constructs (Fig. 18 A-F) indicate the proper fusion to EGFP (no diffuse signal in cytosol and nucleus for EGFP only observed). In terms of localization, expected predominant plasma membrane expression for WT1, WT2 and CS2 mutant was observed. Data acquired with WT1 and WT2 confirm the identity of these two constructs. As expected, mutation affecting interaction with Lck has no effect on sorting of CD4 to the plasma membrane. Lower plasma membrane localization and increased targeting to cytosolic membranes was observed for both CS1 variants (CS1 and RA5CS1). Only RA5 mutant was observed in some cells to accumulate exclusively in the intracellular vesicles with undetectable plasma membrane localization in approximately half of the cells. Remaining RA5 expressing cells show weak plasma membrane and strong cytosolic membrane localization.

Data acquired using mEOS2 fusion proteins (Fig. 19 A-F) again confirmed the successful generation of DNA constructs. In general, CD4-mEos2 transfected cells show lower expression levels and higher accumulation in the intracellular membranes. Individual mutants show similar results as for EGFP fusion constructs with WT1 and WT2 and CS2 mutant predominantly at the plasma membranes, both CS1 variants with increased targeting to cytosolic membranes and RA5 only variants almost exclusive localization to the cytosolic membranes.

Of note, higher transfection efficiency was observed for all DNA constructs when using microporation compared to standard electroporation using aluminum cuvettes.

EGFP

A. CD4wt1

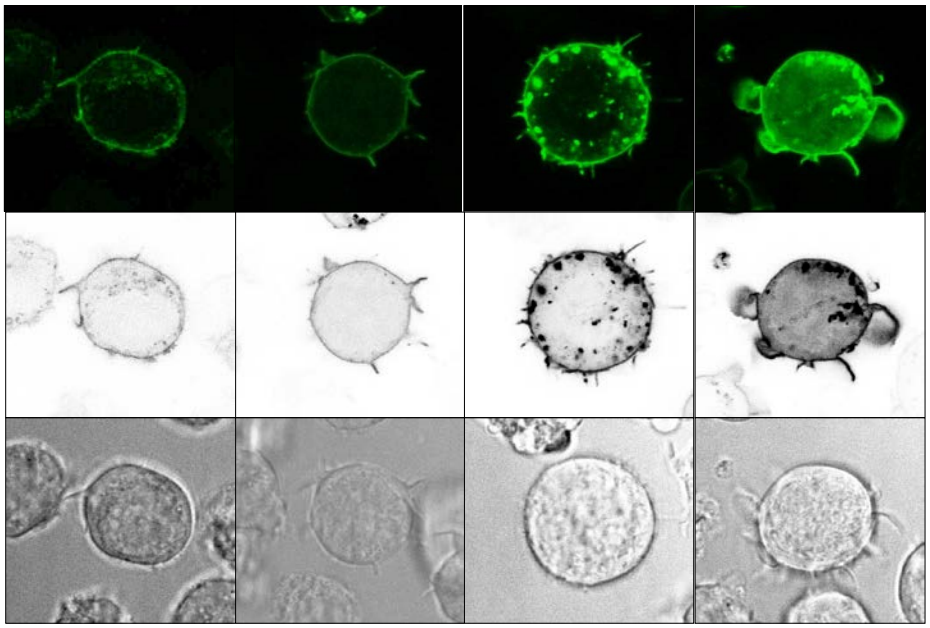

B. CD4wt2

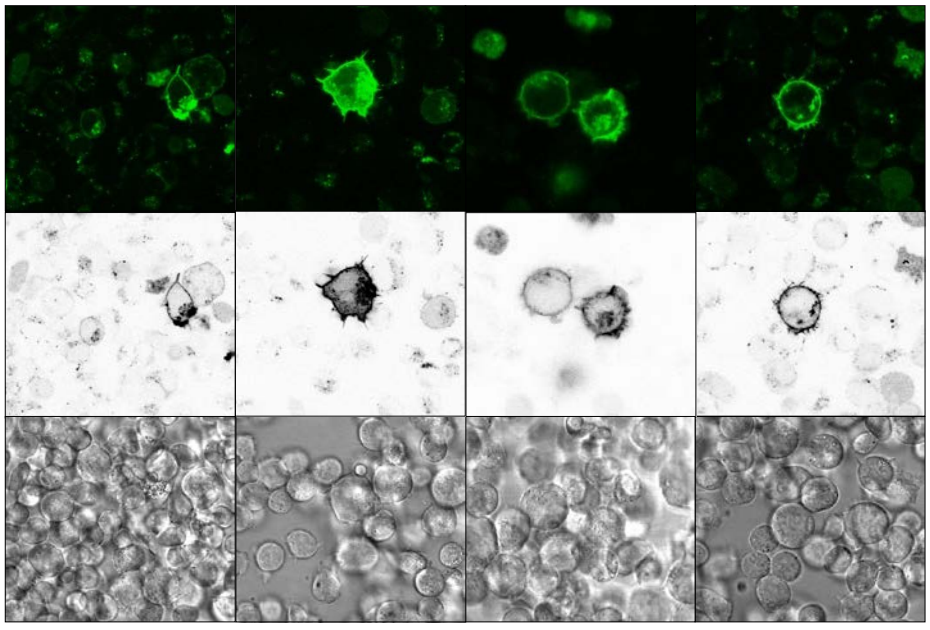

Fig. 18 Confocal microscopy of CD4-EGFP variants in Jurkat cells.
On the top – fluorescence image
In the middle – fluorescence image converted into black and white
On the bottom – brightfield

C. CD4CS1

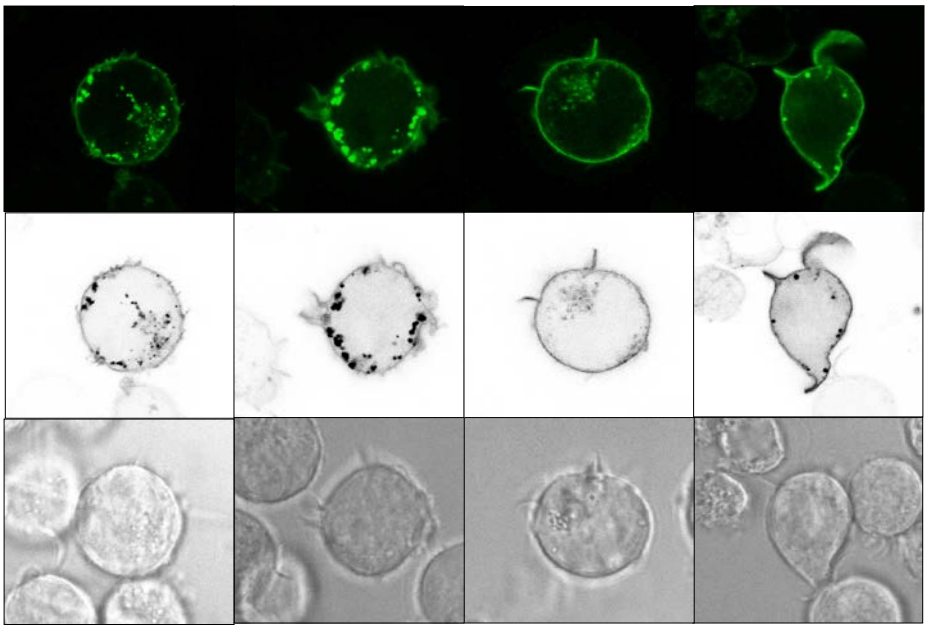

D. CD4CS2

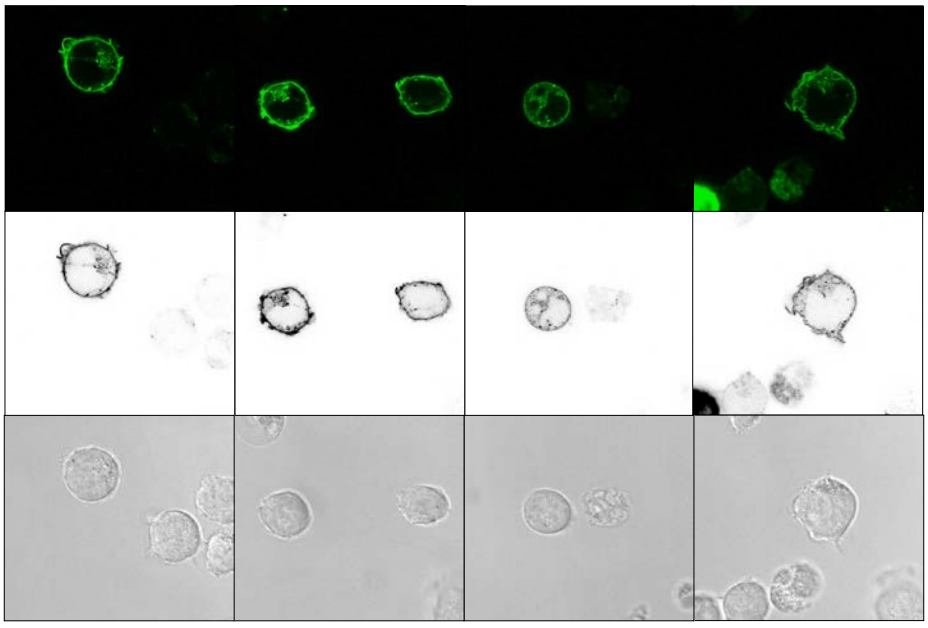

Fig. 18 Confocal microscopy of CD4-EGFP variants in Jurkat cells (continuation).
On the top – fluorescence image
In the middle – fluorescence image converted into black and white
On the bottom – brightfield

E. CD4RA5

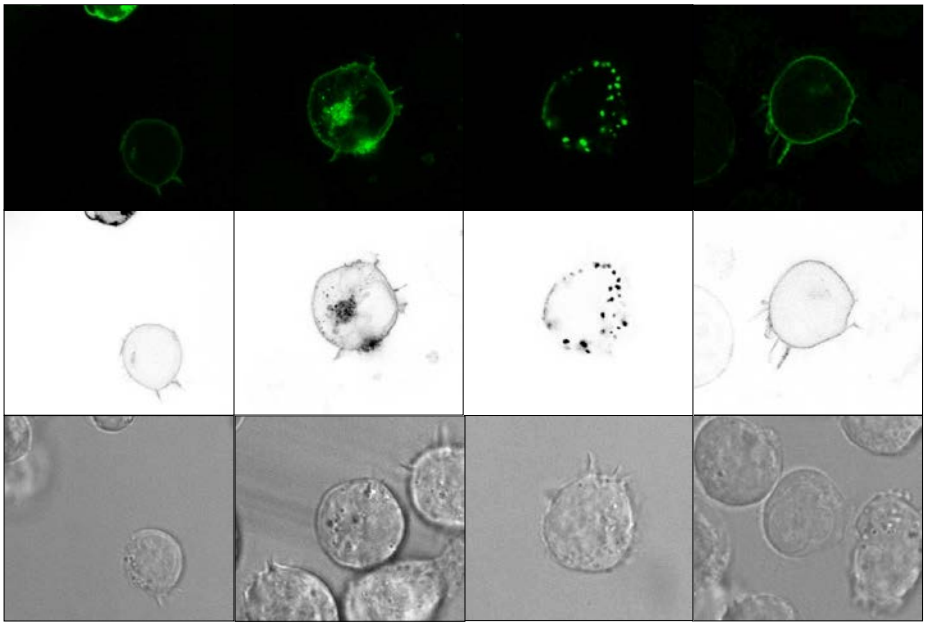

F. CD4RA5CS1

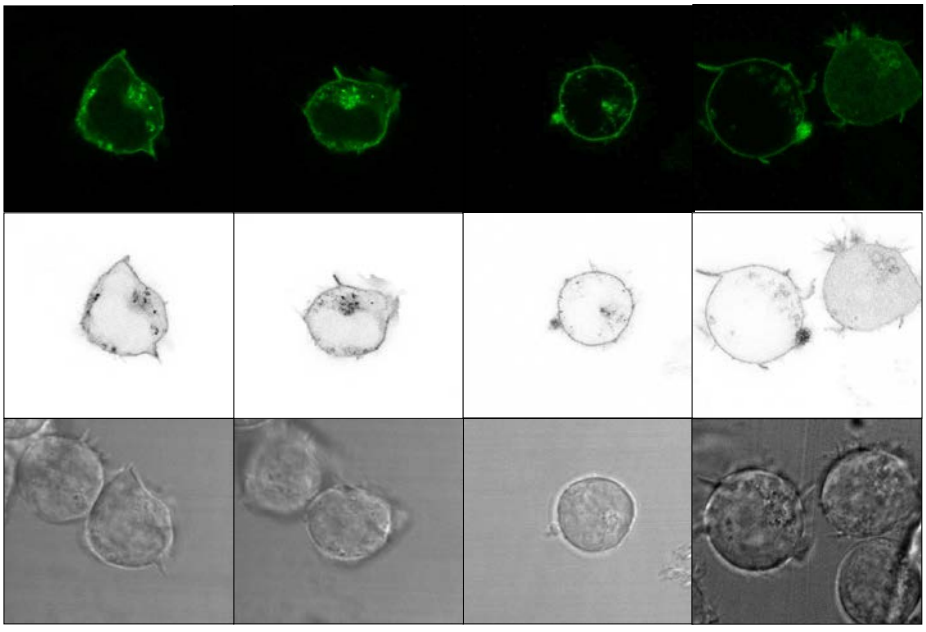

Fig. 18 Confocal microscopy of CD4-EGFP variants in Jurkat cells (continuation).
On the top – fluorescence image
In the middle – fluorescence image converted into black and white
On the bottom – brightfield

mEOS2

A. CD4wt1

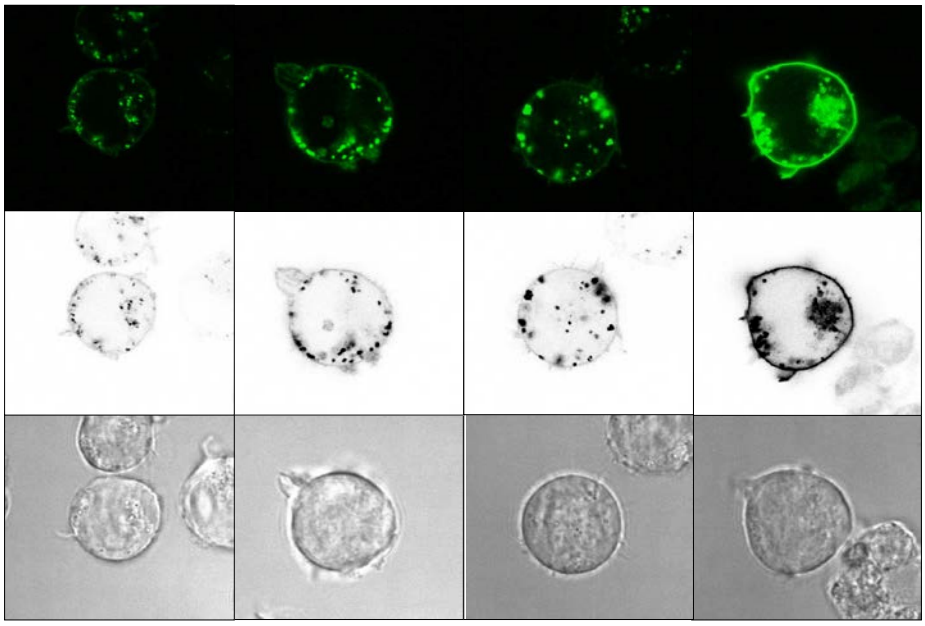

B. CD4wt2

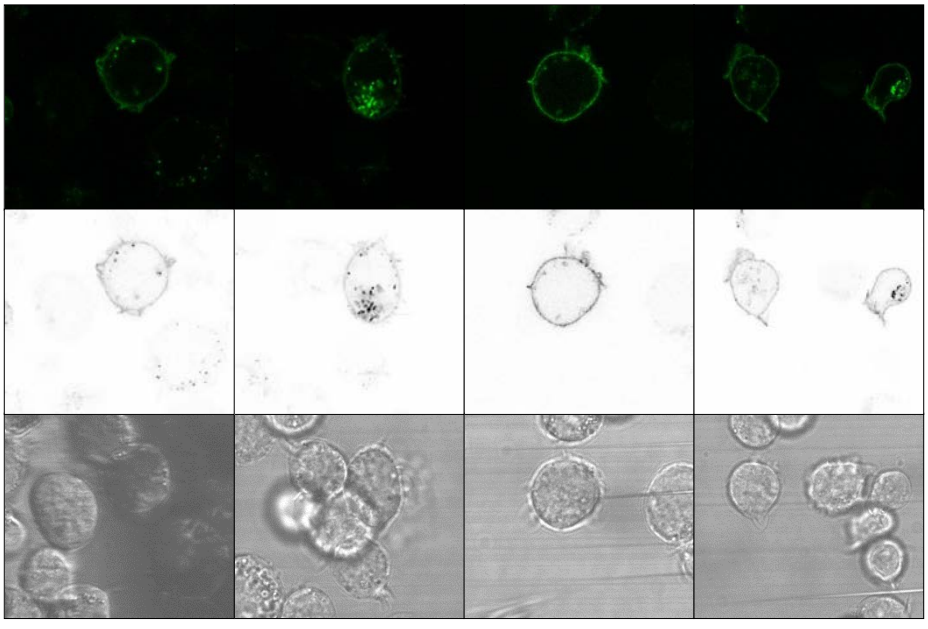

Fig. 19 Confocal microscopy of CD4-mEOS2 variants in Jurkat cells.
On the top – fluorescence image
In the middle – fluorescence image converted into black and white
On the bottom – brightfield

C. CD4CS1

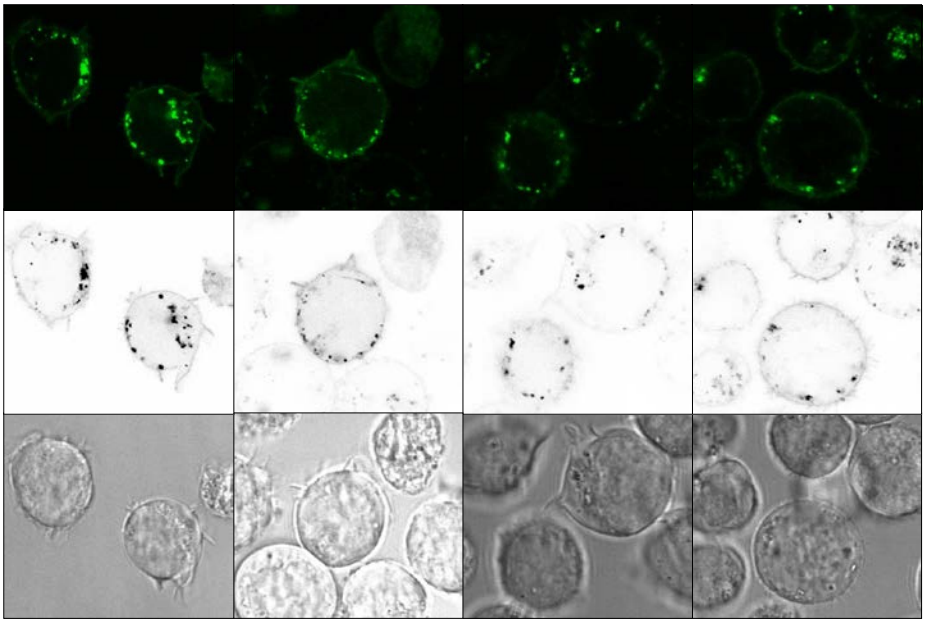

D. CD4CS2

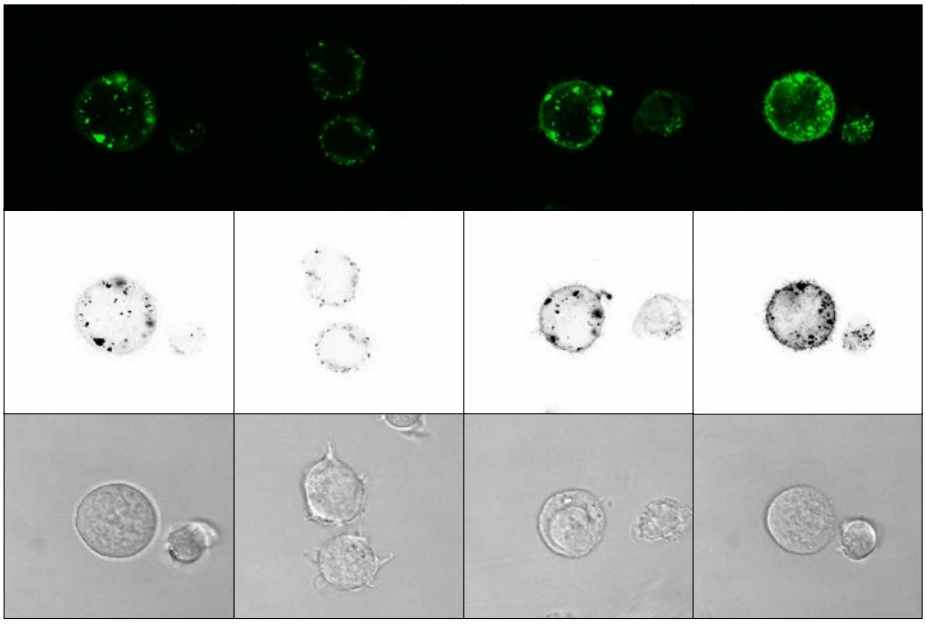

Fig. 19 Confocal microscopy of CD4-mEOS2 variants in Jurkat cells (continuation).

On the top – fluorescence image
In the middle – fluorescence image converted into black and white
On the bottom – brightfield

E. CD4RA5

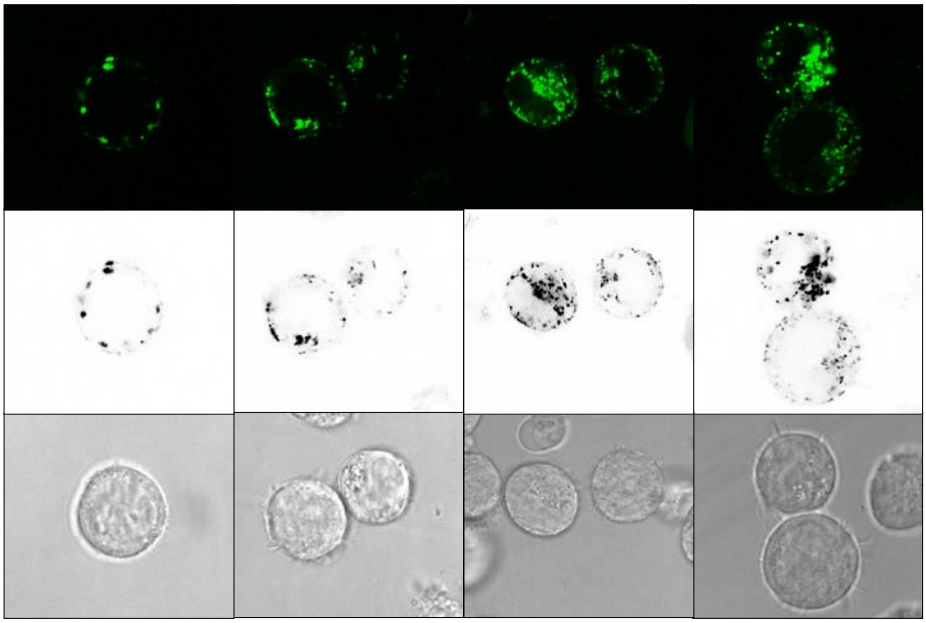

F. CD4RA5CS1

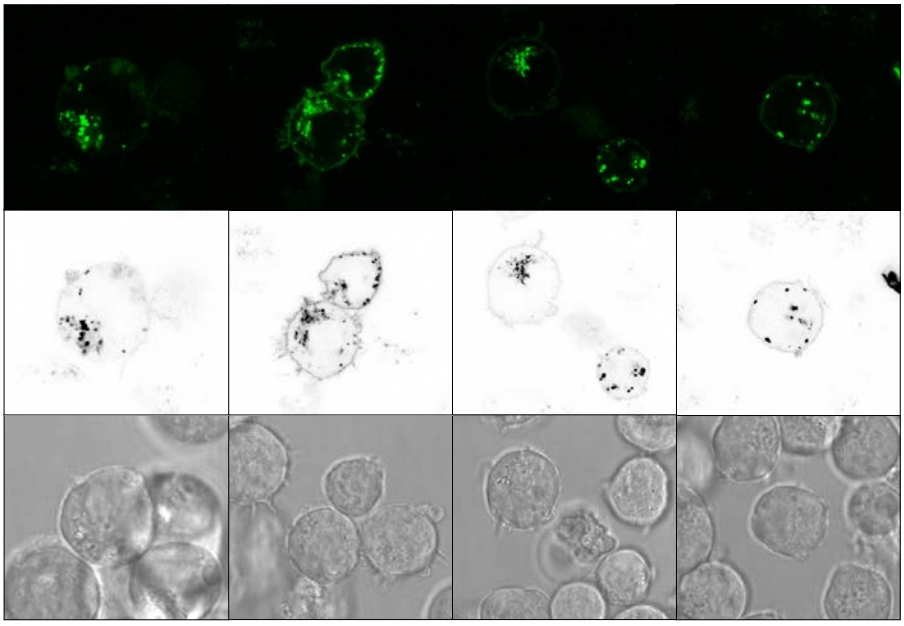

Fig. 19 Confocal microscopy of CD4-mEOS2 variants in Jurkat cells (continuation).
On the top – fluorescence image
In the middle – fluorescence image converted into black and white
On the bottom – brightfield

4.3 Superresolution localization microscopy (PALM) data analysis

Jurkat T cells were transfected with pCD4wt1-mEOS2 and pCD4CS1-mEOS2 plasmids using microporation technique. Next day, transfected cells were activated on OKT3 antibody-coated coverslips for 7 minutes, fixed and subsequently examined by localization microscopy (PALM).

Superresolution imaging of transfected Jurkat T cells was performed using Olympus widefield microscope in TIRF mode at frame rate 30ms/frame. Activation of mEOS2 fluorescence at 561 nm was achieved by UV illumination at 405 nm using low power laser line (approx. 100µW at the objective). 10-20.000 frames were collected to acquire superresolution image.

Number of analyzed cells transfected with pCD4wt1-mEOS2 was n = 12, for pCD4CS1-mEOS2 n = 17. Data acquired for each cell were first processed by ImageJ/FiJi (image processing package; Schindelin et al., 2012) and localizations of single molecule fluorescence events were acquired using rapidSTORM software (Wolter et al., 2010). Examples of superresolution image (in black and white) are shown in (Fig. 20; on the top). For further processing, areas of 3x3 µm were selected from imaged cells (1-3 areas per cell) avoiding cell edge. Localizations from these square fields were analyzed using MATLAB scripts from Dave Williamson and Katharina Gaus (University of New South Wales, Sydney) for cluster analysis (Owen et al., 2012; Tab. 6). Each localization is valued for clustering, using Getis-Franklin´s local point pattern analysis (Getis and Franklin, 1987) which calculates how clustered is individual point (localization) on a 50nm scale. The size of area (50nm radius) was selected since most of the observed clusters are approximately 100nm in size. These values are then used to generate pseudo-3D cluster maps, such as those in (Fig. 20; in the middle). Such maps can be further analyzed to acquire important quantitative information on protein clustering (see below). For this, binary map needs to be generated using user-selected cut-off value to distinguish clusters (black) and non-clustered areas (white). Examples of such binary maps are on (Fig. 20; on the bottom). Clusters in 60 areas for CD4wt1-mEOS2 and 32 for CD4CS1-mEOS2 were tested.

Cluster analysis provides information on number of molecules in each cluster, number of clusters per 1μm^2 area, percentage of area occupied by clusters, average size of clusters (μm^2) and density ratio of molecules in and out of clusters. Results are shown in (Tab. 6) and indicate high clustering for both CD4 variants (CD4wt1-mEOS2 and CD4CS1-mEOS2) under tested conditions.

Analysed area = 9μm^2	**Count (number of clusters in area)**	**Average Size of 1 cluster (μm^2)**	**%Area (occupied by clusters)**	**Clusters/ μm^2**
WT1				
average	55,1	0,009583333	5,82491667	6,122222222
standard deviation	8,564214074	0,002309095	1,47622358	0,951579342
CS1				
average	55,46875	0,00690625	4,26340625	6,163194444
standard deviation	7,157150158	0,001766341	1,10210215	0,795238906
	Total number of molecules in area	**Average number molecules/cluster**	**% molecules in clusters**	**Density ratio (densin/densout)**
WT1				
average	3077,75	30,2720517	58,94817838	25,5037025
standard deviation	2106,069853	14,5274058	12,10526636	7,825136938
CS1				
average	3689,3125	28,6435953	45,61899072	19,86008304
standard deviation	1649,140645	8,54077223	11,79106291	5,207074177

Tab. 6 Cluster analysis data from localization microscopy of WT1 – CD4wt1-mEOS2 and **CS1 –** CD4CS1-mEOS2.

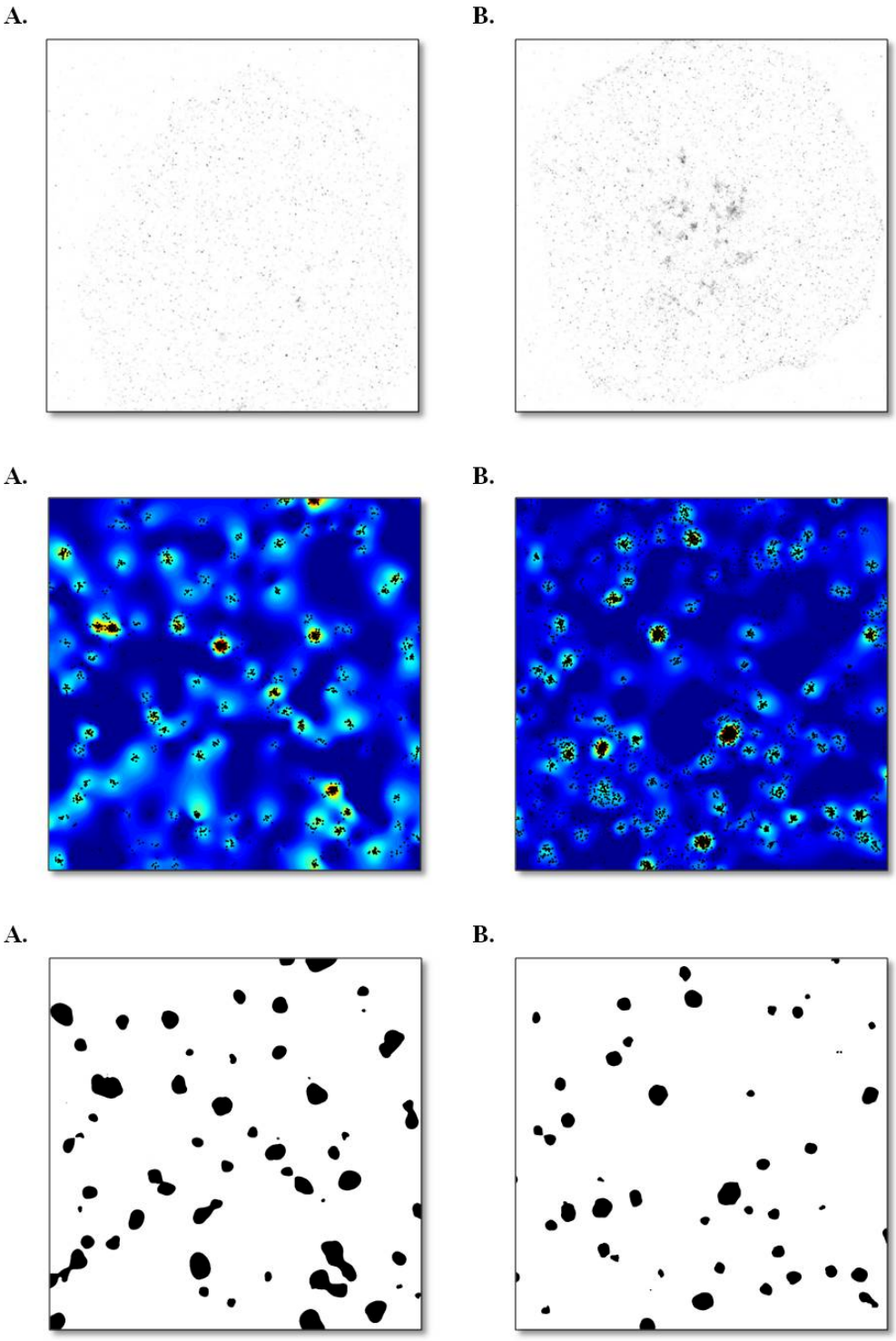

Fig. 20 Localization microscopy data image processing.

A. CD4wt1 – mEOS2

B. CD4CS1 – mEOS2

On the top – example of superresolution image (data processed by Fiji and rapidSTORM software)

In the middle – pseudo-3D cluster maps (data further processed using MATLAB scripts and Getis-Franklin´s local point pattern analysis)

On the bottom – binary map

5 Discussion

The aim of my work was to generate fusion constructs of human CD4 glycoprotein and its mutant forms with fluorescent proteins EGFP and mEOS2, perform proper characterization of all constructs and subsequently provide validation of generated constructs using single molecule localization microscopy (PALM).

CD4 glycoprotein and its mutant variants used in this thesis were kindly donated by Waldemar Popik´s and Stèphane Basmaciogullari´s laboratories. CD4 versions from W.P. (including CD4wt1-EGFP, CD4CS1-EGFP, CD4RA5-EGFP and CD4CS1RA5-EGFP) were already fused with EGFP. EGFP fusion variants were suitable for Western blot analysis and confocal microscopy of fusion proteins whereas for localization microscopy, photoconvertible fluorescence fusion proteins, e.g. mEOS2, are required. Plasmids from S.B. (encoding CD4wt2 and CD4CS2) originally contained no fluorescent protein. Here, both EGFP and mEOS2 fusion variants were prepared and genetically characterized. Sequencing revealed that CD4wt1 and CD4wt2 sequences are identical. When started to work on this thesis, it was uncertain whether these sequences are the same since isoform variants of CD4 were reported in past (Uniprot; P01730). Published isoforms contain charge-change mutations (Lys-Asp) and can influence localization of CD4 molecule or its interaction with binding partners.

Biochemical properties of generated constructs were verified by transfection of constructs into HEK293FT cell line. This cell line was chosen due to high transfection efficiency, a property essential for biochemical characterization. The efficiency of transfection was first tested under the fluorescent microscope. Transfection proved excellent efficiency. All generated constructs demonstrated successful fusion with fluorescent proteins EGFP and/or mEOS2 and capacity to be effectively expressed in human cells. Both EGFP and mEOS2 fluorescent proteins emitted green fluorescence as expected. mEOS2 emission was weaker due to its lower extinction coefficient compared to EGFP (McKinney et al., 2009). In the next step, proper folding and appropriate molecular weight of CD4 constructs were examined using Western blotting method. Staining with antibodies against human CD4 glycoprotein and GFP confirmed correct molecular weight of all generated CD4 constructs. An interesting phenomenon was observed using this method. The correct molecular weight of CD4-EGFP and CD4-mEOS2 constructs are 78kDa and 77kDa, respectively. An additional strong band for the CD4 staining was

detected in the molecular weight corresponding to 55kDa. This molecular weight matches with human CD4 glycoprotein lacking fluorescent fusion protein. During maturation of nascent protein or during transportation to the plasma membrane decomposition of the two parts of fusion protein can happen. The degradation is noticeable in case of both fluorescent fusion variants EGFP and mEOS2. Previously, it has been reported that some fraction of all fluorescent proteins decompose by autocatalytic cleavage before they reach the target location (Craggs, 2009). The reason why this happens is not completely clear. This issue has not been studied intensely to date.

Since the ability of generated constructs to express in human cell line, proper maturation and correct molecular weight were confirmed, we were interested in the localization of CD4 variants in the Jurkat T cell line. A long term goal of my work is single molecule localization microscopy of CD4 variants using PALM TIRFM technique. To achieve this goal, localization of mEOS2 fusion CD4 variants at the plasma membrane is essential. All constructs comply with this condition with one exception of CD4RA5-mEOS2 variant where the noticeable number of transfected cells revealed strong localization to cytosolic membranes but almost undetectable at the surface. CD4wt1, 2 and CD4CS2-EGFP variants mainly accumulated at the plasma membrane whereas CD4CS1 variant demonstrated increased targeting into cytosolic membranes. The common pattern for all mEOS2 constructs was lower expression levels and higher appearance in cytosolic membranes compared to CD4-EGFP variants. On the other hand targeting of CD4-EGFP constructs was similar to those with mEOS2 confirming the impact of mutations on CD4 localization and only lower caused by the fusion with different fluorescent proteins.

Localization microscopy confirmed proper function of mEOS2 in tested fusion proteins (UV photoconversion). In addition, preliminary cluster analysis of CD4wt1-mEOS2 and CD4CS1-mEOS2 was performed. There is relevant difference in clustering of these two proteins. Actually, values for clusters per μm^2, average number of molecules per cluster were almost identical indicating formation of similar clusters. On the other hand, small reduction on average cluster size and percentage of molecules in clusters was detected. This could mean that palmitoylation can influence size of CD4 clusters but it is not essential for clustering per se. This is also expressed in density ratio. Comparing density of CD4 molecules in clusters versus in non-clustered areas again indicate weaker clustering of non-palmitoyled CD4 mutant variant (CD4CS1-mEOS2) to their CD4wt1-mEOS2 counterparts. Remaining CD4 variants haven´t been evaluated by localization microscopy due to time-intense experiment required for proper cluster analysis.

Further investigation of all CD4 variants using localization microscopy is required to better understand the role of CD4 during the early phase of T cell activation. CD4 and its mutant variants potentially causing its different localization at the membrane will be colocalized with TCR and effector kinase Lck and membrane organization changes will be investigated imaging various time points of T cell activation as well as employing live cell imaging to learn more about CD4 dynamics in the immunological synapse.

6 Conclusion

In this thesis, recombinant DNA plasmids encoding CD4 and its variants in form of fluorescent fusion proteins were prepared and characterized. Biochemical analysis provided information on appropriate expression and size of the recombinant proteins. Confocal microscopy further approved correct folding of studied fusion proteins and their localization pattern in T cells. All CD4 variants localized to the plasma membrane of Jurkat T cells except of CD4 basic-rich domain mutant variant which accumulated mainly in the intracellular membranes with weak plasma membrane expression. Unlike other variants, wild-type and palmitoylation mutant were tested for localization microscopy using fusion with photoconvertible fluorescent protein mEOS2. The data indicate similar level of clustering of these two variants at the surface of activated T cells. All constructs will be further characterized in detailed localization microscopy study to uncover any changes in membrane CD4 organization caused by mutations in the intracellular part. It is very likely that examination of the rest of available CD4 mutant variants in colocalization with TCR, Lck or other proteins participating on T cell activation such as polymerized actin will also improve our knowledge about the role of CD4 during TCR triggering of T cell activation.

7 List of abbreviations

APC	-	antigen presenting cell
BCR	-	B cell receptor
CD	-	cluster of differentiation
dNTP	-	deoxyribonucleotide triphosphate
FACS	-	Fluorescence-activated cell sorting
GFP	-	green fluorescent protein
HIV	-	human immunodeficiency virus
ICAM1	-	intracellular adhesion molecule 1
IFNγ	-	interferon γ
Ig	-	immunoglobulin
IL	-	interleukin
IS	-	immunological synapse
ITAM	-	Immunoreceptor tyrosine-based activation motif
LAT	-	linker of activated T cells
LBPA	-	Lysobisphosphatidic acid
Lck	-	lymphocyte-specific protein tyrosine kinase
LFA-1	-	leukocyte function-associated molecule-1
MC	-	microcluster
mEOS2	-	Green to red photoconvertible protein EosFP
MHCI	-	major histocompatibility class I
MHCII	-	major histocompatibility class II
p-MHC	-	protein-major histocompatibility complex
PALM	-	photoactivated localization microscopy
PCR	-	polymerase chain reaction
PFA	-	paraformaldehyde
PLC-γ	-	phospholipase C-γ
PCR	-	polymerase chain reaction
PS-CFP2	-	Cyan-to-green photoswitchable fluorescent protein
SH2	-	Src homology 2
SLP-76	-	SH2 domain-containing leukocyte protein of 76kDa

SMAC (c,d,p)	-	supramolecular activation clusters (central, distal, peripheral)
STED	-	stimulated emission depletion microscopy
STORM	-	stochastic optical reconstruction microscopy
TAP	-	transporters associated with antigen processing
TCR	-	T cell receptor
TGFβ	-	tumor growth factor β
T_H1	-	T helper cell type 1
T_H2	-	T helper cell type 2
T_H17	-	T helper cell type 17
TIRFM	-	total internal reflection fluorescence microscopy
TNFα	-	tumor necrosis factor α
TNFβ	-	tumor necrosis factor β
T_{reg}	-	regulatory T cell
ZAP-70	-	Zeta-chain-associated protein kinase 70

8 References

Axelrod D. Cell-substrate contacts illuminated by total internal reflection fluorescence. *J Cell Biol.* 1981;89(1):141-5.

Betzig E, Patterson GH, Sougrat R, Lindwasser OW, Olenych S, Bonifacino JS, Davidson MW, Lippincott-Schwartz J, Hess HF. Imaging intracellular fluorescent proteins at nanometer resolution. *Science.* 2006;313(5793):1642-5.

Boniface JJ, Rabinowitz JD, Wülfing C, Hampl J, Reich Z, Altman JD, Kantor RM, Beeson C, McConnell HM, Davis MM. Initiation of signal transduction through the T cell receptor requires the multivalent engagement of peptide/MHC ligands. *Immunity*. 1998;9(4):459-66.

Brunner T, Wasem C, Torgler R, Cima I, Jakob S, Corazza N. Fas (CD95/Apo-1) ligand regulation in T cell homeostasis, cell-mediated cytotoxicity and immune pathology. *Semin Immunol*. 2003;167–176.

Call ME, Pyrdol J, Wiedmann M, Wucherpfennig KW. The organizing principle in the formation of the T cell receptor-CD3 complex. *Cell.* 2002;111(7):967-79.

Call ME, Wucherpfennig KW. Common themes in the assembly and architecture of activating immune receptors. *Nat Rev Immunol.* 2007;7(11):841-50.

Cebecauer M, Guillaume P, Mark S, Michielin O, Boucheron N. CD8+ cytotoxic T lymphocyte activation by soluble major histocompatibility complex-peptide dimers. *J. Biol. Chem.* 2005;280:23820–28

Chudakov DM, Verkhusha VV, Staroverov DB, Souslova EA, Lukyanov S, Lukyanov KA. Photoswitchable cyan fluorescent protein for protein tracking. *Nat Biotechnol.* 2004;22(11):1435-9.

Craggs TD. Green fluorescent protein: structure, folding and chromophore maturation. *Chem Soc Rev.* 2009;38(10):2865-75.

Cresswell P, Howard JC. Antigen recognition. *Curr Opin Immunol*. 1997;9(1):71-4.

Crise B, Rose JK. Identification of palmitoylation sites on CD4, the human immunodeficiency virus receptor. *J Biol Chem.* 1992;267(19):13593-7.

Douglass AD, Vale RD. Single-molecule microscopy reveals plasma membrane microdomains created by protein-protein networks that exclude or trap signaling molecules in T cells. *Cell.* 2005;121(6):937-50.

Drutskaya MS, Efimov GA, Kruglov AA, Kuprash DV, Nedospasov SA. Tumor necrosis factor, lymphotoxin and cancer. *IUBMB Life*. 2010;62(4):283-9.

Dustin ML, T-cell activation through immunological synapses and kinapses. *Immunol Rev.* 2008;221:77-89.

Dustin ML, Bromley SK, Kan Z, Peterson DA, Unanue ER. Antigen receptor engagement delivers a stop signal to migrating T lymphocytes. *Proc Natl Acad Sci U S A.* 1997;94(8):3909-13.

Dustin ML, Depoil D. New insights into the T cell synapse from single molecule techniques. *Nat Rev Immunol*. 2011;11(10):672-84.

Ehrlich LI, Ebert PJ, Krummel MF, Weiss A, Davis MM. Dynamics of p56lck translocation to the T cell immunological synapse following agonist and antagonist stimulation. *Immunity.* 2002;17(6):809-22.

Fehérvari Z, Sakaguchi S. CD4+ Tregs and immune control. *J Clin Invest.* 2004;114(9):1209-17.

Fragoso R, Ren D, Zhang X, Su MW, Burakoff SJ, Jin YJ. Lipid raft distribution of CD4 depends on its palmitoylation and association with Lck, and evidence for CD4-induced lipid raft aggregation as an additional mechanism to enhance CD3 signaling. *J Immunol*. 2003;170(2):913-21.

Freiberg BA, Kupfer H, Maslanik W, Delli J, Kappler J, Zaller DM, Kupfer A. Staging and resetting T cell activation in SMACs. *Nat Immunol.* 2002;3(10):911-7.

Getis A, Franklin J. Second-order neighborhood analysis of mapped point patterns. Ecology. 1987;68(3):473-477.

Giblin PA, Leahy DJ, Mennone J, Kavathas PB. The role of charge and multiple faces of the CD8 alpha/alpha homodimer in binding to major histocompatibility complex class I molecules: support for a bivalent model. *Proc Natl Acad Sci U S A.* 1994;91(5):1716-20.

Glimcher LH, Murphy KM. Lineage commitment in the immune system: the T helper lymphocyte grows up. *Genes Dev.* 2000;14(14):1693-711.

Grakoui A, Bromley SK, Sumen C, Davis MM, Shaw AS, Allen PM, Dustin ML. The immunological synapse: a molecular machine controlling T cell activation. *Science.* 1999;285(5425):221-7.

Griffiths GM. The cell biology of CTL killing. *Curr Opin Immunol.* 1995;7:343-348.

Hell SW, Wichmann J. Breaking the diffraction resolution limit by stimulated emission: stimulated-emission-depletion fluorescence microscopy. *Opt Lett.* 1994;19(11):780-2.

Hořejší V, Bartůňková J. Základy imunologie. 3.vydání. Praha: *Triton.* 2005;21-44. ISBN 80-7254-686-4.

Huang B, Babcock H, Zhuang X. Breaking the diffraction barrier: super-resolution imaging of cells. *Cell.* 2010;143(7):1047-58.

Irvine DJ, Purbhoo MA, Krogsgaard M, Davis MM. Direct observation of ligand recognition by T cells. *Nature*. 2002;419:845–49

Jacobelli J, Andres PG, Boisvert J, Krummel MF. New views of the immunological synapse: variations in assembly and function. *Curr Opin Immunol*. 2004;16(3):345-52.

Janeway CAJ. The T cell receptor as a multicomponent signaling machine: CD4/CD8 coreceptors and CD45 in T cell activation. *Annu. Rev. Immunol*. 1992;10:645–74

Koretzky GA, Picus J, Thomas ML, Weiss A. Tyrosine phosphatase CD45 is essential for coupling T-cell antigen receptor to the phosphatidyl inositol pathway. *Nature.* 1990;346(6279):66-8.

Koyanagi M, Kerns JA, Chung L, Zhang Y, Brown S, Moldoveanu T, Malik HS, Bix M. Diversifying selection and functional analysis of interleukin-4 suggests antagonism-driven evolution at receptor-binding interfaces. *BMC Evol Biol.* 2010;10:223.

Krogsgaard M, Li QJ, Sumen C, Huppa JB, Huse M, Davis MM. Agonist/endogenous peptide-MHC heterodimers drive T cell activation and sensitivity. *Nature.* 2005;434:238-43.

Krummel MF, Sjaastad MD, Wülfing C, Davis MM. Differential clustering of CD4 and CD3zeta during T cell recognition. *Science.* 2000;289:1349-52.

Kupfer A, Singer SJ, Janeway CA Jr, Swain SL. Coclustering of CD4 (L3T4) molecule with the T-cell receptor is induced by specific direct interaction of helper T cells and antigen-presenting cells. *Proc Natl Acad Sci U S A.* 1987;84(16):5888-92.

Laguette N, Brégnard C, Bouchet J, Benmerah A, Benichou S, Basmaciogullari S. Nef-induced CD4 endocytosis in human immunodeficiency virus type 1 host cells: role of p56lck kinase. *J Virol*. 2009;83(14):7117-28.

Laky K, Fowlkes BJ. Receptor signals and nuclear events in CD4 and CD8 T cell lineage commitment. *Curr Opin Immunol.* 2005;17(2):116-21.

Leahy DJ. A structural view of CD4 and CD8. *FASEB J.* 1995;9(1):17-25.

Lillemeier BF, Mörtelmaier MA, Forstner MB, Huppa JB, Groves JT, Davis MM. TCR and Lat are expressed on separate protein islands on T cell membranes and concatenate during activation. *Nat Immunol.* 2010;11(1):90-6.

Luckheeram RV, Zhou R, Verma AD, Xia B. $CD4^{+}$T cells: differentiation and functions. *Clin Dev Immunol.* 2012;2012:925135.

Manolios N, Ali M, Bender V. T-cell antigen receptor (TCR) transmembrane peptides: A new paradigm for the treatment of autoimmune diseases. *Cell Adh Migr*. 2010;4(2):273-83.

McKinney SA, Murphy CS, Hazelwood KL, Davidson MW, Looger LL. A bright and photostable photoconvertible fluorescent protein. *Nat Methods.* 2009;6(2):131-3.

Melkonian KA, Ostermeyer AG, Chen JZ, Roth MG, Brown DA. Role of lipid modifications in targeting proteins to detergent-resistant membrane rafts. Many raft proteins are acylated, while few are prenylated. *J Biol Chem*. 1999;274(6):3910-7.

Morley SC, Sung J, Sun GP, Martelli MP, Bunnell SC, Bierer BE. Gelsolin overexpression alters actin dynamics and tyrosine phosphorylation of lipid raft-associated proteins in Jurkat T cells. *Mol Immunol.* 2007;44(9):2469-80.

Murphy K, Travers P, Walport M. Janeway´s immunobiology. 7th edition**.** New York: *Garland Science*. 2008;323-416. ISBN 978-0-8153-4123-9.

Negulescu PA, Krasieva TB, Khan A, Kerschbaum HH, Cahalan MD. Polarity of T cell shape, motility, and sensitivity to antigen. *Immunity.* 1996;4(5):421-30.

Nunès JA, Battifora M, Woodgett JR, Truneh A, Olive D, Cantrell DA. CD28 signal transduction pathways. A comparison of B7-1 and B7-2 regulation of the map kinases: ERK2 and Jun kinases. *Mol Immunol.* 1996;33(1):63-70.

Okoye IS, Wilson MS. CD4+ T helper 2 cells--microbial triggers, differentiation requirements and effector functions. *Immunology*. 2011;134(4):368-77.

Owen DM, Gaus K, Magee AI, Cebecauer M. Dynamic organization of lymphocyte plasma membrane: lessons from advanced imaging methods. *Immunology.* 2010;131(1):1-8.

Owen DM, Williamson D, Magenau A, Gaus K. Optical techniques for imaging membrane domains in live cells (live-cell PALM of protein clustering). *Methods Enzymol.* 2012;504:221-35.

Popik W, Alce TM. CD4 receptor localized to non-raft membrane microdomains supports HIV-1 entry. Identification of a novel raft localization marker in CD4. *J Biol Chem.* 2004;279(1):704-12.

Roncarolo MG, Bacchetta R, Bordignon C, Narula S, Levings MK. Type 1 T regulatory cells. *Immunol Rev.* 2001;182:68-79.

Rossy J, Owen DM, Williamson DJ, Yang Z, Gaus K. Conformational states of the kinase Lck regulate clustering in early T cell signaling. *Nat Immunol.* 2013;14(1):82-9.

Rudd CE, Anderson P, Morimoto C, Streuli M, Schlossman SF. Molecular interactions, T-cell subsets and a role of the CD4/CD8:p56lck complex in human T-cell activation. *Immunol Rev.* 1989;111:225-66.

Rust MJ, Bates M, Zhuang X. Sub-diffraction-limit imaging by stochastic optical reconstruction microscopy (STORM). *Nat Methods.* 2006;3(10):793-5.

Sattentau QJ, Moore JP. The role of CD4 in HIV binding and entry. *Philos Trans R Soc Lond B Biol Sci.* 1993;342:59-66.

Sherman E, Barr V, Manley S, Patterson G, Balagopalan L, Akpan I, Regan CK, Merrill RK, Sommers CL, Lippincott-Schwartz J, Samelson LE. Functional nanoscale organization of signaling molecules downstream of the T cell antigen receptor. *Immunity.* 2011;35(5):705-20.

Schindelin J, Arganda-Carreras I, Frise E, Kaynig V, Longair M, Pietzsch T, Preibisch S, Rueden C, Saalfeld S, Schmid B, Tinevez JY, White DJ, Hartenstein V, Eliceiri K, Tomancak P, Cardona A. FiJi: an open-source platform for biological-image analysis. *Nat Methods.* 2012 Jun 28;9(7):676-82.

Schraven B, Marie-Cardine A, Hübener C, Bruyns E, Ding I. Integration of receptor-mediated signals in T cells by transmembrane adaptor proteins. *Immunol Today.* 1999;20(10):431-4.

Spörri R, Reis e Sousa C. Self peptide/MHC class I complexes have a negligible effect on the response of some CD8+ T cells to foreign antigen. *Eur J Immunol*. 2002;32(11):3161-70.

Straus DB, Weiss A. Genetic evidence for the involvement of the lck tyrosine kinase in signal transduction through the T cell antigen receptor. *Cell.* 1992;70(4):585-93.

Varma R, Campi G, Yokosuka T, Saito T, Dustin ML. T cell receptor-proximal signals are sustained in peripheral microclusters and terminated in the central supramolecular activation cluster. *Immunity.* 2006;25(1):117-27.

Veillette A, Bookman MA, Horak EM, Bolen JB. The CD4 and CD8 T cell surface antigens are associated with the internal membrane tyrosine-protein kinase p56lck. *Cell.* 1988;55(2):301-8.

Waterhouse NJ, Clarke CJP, Sedelies KA, Teng MW, Trapani JA. Cytotoxic lymphocytes; instigators of dramatic target cell death. *Biochem Pharmacol.* 2004;68(6):1033-40.

Weenink SM, Gautam AM. Antigen presentation by MHC class II molecules. *Immunol Cell Biol.* 1997;75(1):69-81.

Weiss A. Structure and function of the T cell antigen receptor. *J Clin Invest*. 1990; 86(4): 1015–1022.

Wilson IA, Fremont DH. Structural analysis of MHC class I molecules with bound peptide antigens. *Semin Immunol.* 1993;5(2):75-80.

Wolter S, Schüttpelz M, Tscherepanow M, VAN DE Linde S, Heilemann M, Sauer M. Real-time computation of subdiffraction-resolution fluorescence images. *J Microsc.* 2010;237(1):12-22.

Yin Y, Wang XX, Mariuzza RA. Crystal structure of a complete ternary complex of T-cell receptor, peptide-MHC, and CD4. *Proc Natl Acad Sci U S A.* 2012;109(14):5405-10.

Yokosuka T, Sakata-Sogawa K, Kobayashi W, Hiroshima M, Hashimoto-Tane A, Tokunaga M, Dustin ML, Saito T. Newly generated T cell receptor microclusters initiate and sustain T cell activation by recruitment of Zap70 and SLP-76. *Nat Immunol.* 2005;6(12):1253-62.

Zamoyska R. CD4 and CD8: modulators of T-cell receptor recognition of antigen and of immune responses? *Curr Opin Immunol*. 1998;10(1):82-7.

Internet sources:

http://www.basic.northwestern.edu/biotools/oligocalc.html
http://www.www.seqme.eu
http://www.uniprot.org